Biogeosciences, 12, 6125–6146, 2015
www.biogeosciences.net/12/6125/2015/
doi:10.5194/bg-12-6125-2015

Biogeosciences Open Access EGU

A strong CO_2 sink enhanced by eutrophication in a tropical coastal embayment (Guanabara Bay, Rio de Janeiro, Brazil)

L. C. Cotovicz Jr.[1,2], **B. A. Knoppers**[1], **N. Brandini**[1], **S. J. Costa Santos**[1], **and G. Abril**[1,2]

[1]Programa de Geoquímica, Universidade Federal Fluminense, Outeiro São João Batista s/n, 24020015, Niterói, RJ, Brazil
[2]Laboratoire Environnements et Paléoenvironnements Océaniques et Continentaux (EPOC), CNRS, Université de Bordeaux, Allée Geoffroy Saint-Hilaire, 33615 Pessac Cedex, France

Correspondence to: L. C. Cotovicz Jr. (lccjunior@id.uff.br)

Received: 3 February 2015 – Published in Biogeosciences Discuss.: 23 March 2015
Revised: 9 September 2015 – Accepted: 9 October 2015 – Published: 27 October 2015

Abstract. In contrast to its small surface area, the coastal zone plays a disproportionate role in the global carbon cycle. Carbon production, transformation, emission and burial rates at the land–ocean interface are significant at the global scale but still poorly known, especially in tropical regions. Surface water pCO_2 and ancillary parameters were monitored during nine field campaigns between April 2013 and April 2014 in Guanabara Bay, a tropical eutrophic to hypertrophic semi-enclosed estuarine embayment surrounded by the city of Rio de Janeiro, southeast Brazil. Water pCO_2 varied between 22 and 3715 ppmv in the bay, showing spatial, diurnal and seasonal trends that mirrored those of dissolved oxygen (DO) and chlorophyll *a* (Chl *a*). Marked pCO_2 undersaturation was prevalent in the shallow, confined and thermally stratified waters of the upper bay, whereas pCO_2 oversaturation was restricted to sites close to the small river mouths and small sewage channels, which covered only 10 % of the bay's area. Substantial daily variations in pCO_2 (up to 395 ppmv between dawn and dusk) were also registered and could be integrated temporally and spatially for the establishment of net diurnal, seasonal and annual CO_2 fluxes. In contrast to other estuaries worldwide, Guanabara Bay behaved as a net sink of atmospheric CO_2, a property enhanced by the concomitant effects of strong radiation intensity, thermal stratification, and high availability of nutrients, which promotes phytoplankton development and net autotrophy. The calculated CO_2 fluxes for Guanabara Bay ranged between −9.6 and −18.3 mol C m^{-2} yr^{-1}, of the same order of magnitude as the organic carbon burial and organic carbon inputs from the watershed. The positive and high net community production (52.1 mol C m^{-2} yr^{-1}) confirms the high carbon production in the bay. This autotrophic metabolism is apparently enhanced by eutrophication. Our results show that global CO_2 budgetary assertions still lack information on tropical, marine-dominated estuarine systems, which are affected by thermal stratification and eutrophication and behave specifically with respect to atmospheric CO_2.

1 Introduction

The increase in atmospheric CO_2 concentrations in the last decades is of global concern, mainly due to global atmospheric temperature increases (Allen et al., 2009; Matthews et al., 2009) and ocean acidification (Doney et al., 2009). The oceans are known to act as the major sink of atmospheric CO_2, with well-quantified air–sea exchange and uptake of excess anthropogenic CO_2 (Takahashi et al., 2002; Sabine et al., 2004; Orr et al., 2005). The coastal ocean, however, is still subject to controversy and is poorly understood due to its intrinsic intra- and inter-specific heterogeneity. Some of the reasons for these uncertainties include the lack of sufficient studies covering the spatial and temporal variability with a common standardized sampling strategy and methodology and the manifold diverse ecosystem types (estuaries, deltas, embayments and coastal lagoons) affected by multiple external and internal sources (Gattuso et al., 1998; Borges, 2005; Chen et al., 2013; Cloern et al., 2014). Despite the small surface area of the coastal ocean of about 7 % of the global ocean, it exerts a disproportionately large influence upon the carbon cycle, especially on the role of primary production, remineralization and sedimentation of organic matter (Gat-

tuso et al., 1998; Wollast, 1998). Coastal ecosystems receive material from land via river inputs, submerged groundwater discharge, and atmospheric deposition, as well as from the adjacent open ocean. The climatological regime has great influence over these areas, and contributes to the great variability in biogeochemical processes in space and time. In addition, approximately 37 % of the human population lives within 100 km of the coastline (Cohen et al., 1997), making this area subject to intense human impact upon the marine environment, including enhanced loading of nutrients, suspended matter, organic and inorganic matter with associated pollutants, and also overfishing (Bauer et al., 2013).

Several authors have demonstrated that the CO_2 emissions from estuaries are globally significant (Borges and Abril, 2011; Chen et al., 2013). Total ecosystem respiration generally exceeds gross primary production in most estuaries (Gattuso et al., 1998), which are net heterotrophic and sources of atmospheric CO_2 (Borges and Abril, 2011; Cloern et al., 2014). The Land-Ocean Interactions in the Coastal Zone (LOICZ) programme budgetary assertions of more than 250 estuaries and lagoons have also shown that most of them are heterotrophic or may have a balanced metabolism (Knoppers, 1994; Smith et al., 2010). CO_2 outgassing in most sectors of the estuaries is supported by the inputs of CO_2-enriched freshwaters, as well as by the CO_2 generated in the estuarine system itself, by planktonic and benthic net heterotrophy, and by CO_2 advection from salt marshes and mangroves (e.g. Borges and Abril, 2011; Cai, 2011). On the other hand, low-pCO_2 waters and autotrophic metabolism have been observed in some estuarine plumes but with a small percentage of the surface area when compared to the freshwater influence (Borges and Abril, 2011). As more systems are being included in the budgeting effort, the global estuarine CO_2 emission estimate at the air–water interface has been declining (Borges and Abril, 2011; Guo et al., 2012; Chen et al., 2013; Huang et al., 2015). The pioneer estimate of the CO_2 released by estuaries was 0.51 Pg C yr^{-1} (Borges, 2005) and the latest estimate has been adjusted to 0.094 Pg C yr^{-1}. (Chen et al., 2013). In fact, the first budgets were based on data in systems generally located in temperate regions which were river-dominated, macrotidal and turbid (Borges, 2005; Borges and Abril, 2011). The more recent estimate includes a set of new data from estuaries located in low-wind regions and the Arctic Ocean, which contributed to the decrease in the carbon released (Chen et al., 2013). Additionally, Jiang et al. (2008) demonstrated that pCO_2 can be significantly lower in marine-dominated estuaries than river-dominated ones, and according to Maher and Eyre (2012), marine-dominated estuaries with low freshwater influences can be CO_2 sinks.

In tropical regions, the spatial coverage of CO_2 fluxes of estuaries is still scarce. However, the limited number of available studies suggest that tropical estuaries are generally sources of CO_2 to the atmosphere (Souza et al., 2009; Sarma et al., 2012; Araujo et al., 2014), with the exception of one lagoon (Koné et al., 2009). Also, most studies are potentially biased by the lack of information on the diurnal variations in CO_2, which corresponds to a crucial component of mass balance calculations (Borges and Frankignoulle, 1999; Zhang et al., 2013; Maher et al., 2015).

The CO_2 budgets of coastal ecosystems may also be altered by eutrophication generated by the anthropogenic nutrient inputs from sewage and fertilizer usage in agriculture, which has become a widespread water quality issue (Nixon, 1995; Cloern, 2001). The consequences of eutrophication, like the development of excessive algal blooms, toxic algae, loss of submerged aquatic vegetation and increase in hypoxia and anoxia, have been well documented (Bricker et al., 2003; Rabalais et al., 2009). However, the influence of eutrophication per se on the CO_2 budgets is poorly documented. In fact, the response of estuarine metabolism to eutrophication seems to be system-type-specific. Some papers have determined that eutrophication can amplify autotrophy and favour CO_2 uptake (Gypens et al., 2009), while others have shown that eutrophication can reinforce heterotrophy and CO_2 degassing (Sarma et al., 2012; Chou et al., 2013; Wallace et al., 2014).

The present study addresses the question of whether a tropical, marine-dominated, and eutrophic estuarine system – Guanabara Bay (southeast Brazil) – is a sink or a source of atmospheric CO_2. The bay, surrounded by the city of Rio de Janeiro, is the second largest Brazilian estuarine embayment (Kjerfve et al., 1997). The system is one of the most degraded estuaries worldwide. The waters of Guanabara are eutrophic to hypertrophic (according to the classification of Nixon, 1995) and provide ideal conditions to assess the response of aquatic CO_2 metabolism under marked eutrophication. CO_2 fluxes at the air–water interface of Guanabara Bay were estimated with continuous monitoring of surface water pCO_2, taking into account different temporal (daily and seasonal) and spatial scales. Our results show a very different behaviour in terms of carbon cycling of Guanabara Bay compared to previously documented estuaries, with extremely low values of pCO_2 and a net uptake of atmospheric CO_2 annually.

2 Material and methods

2.1 Study site

Guanabara Bay (22°41′–22°58′ S, 43°02′–43°18′ W) is located on the southeastern coast of Brazil, in the southwest Atlantic, and embedded within the metropolitan area of Rio de Janeiro, the second most densely populated region of the Brazilian coast (Fig. 1). The bay has a surface area of 384 km^2, a mean depth of about 5.7 m, and a volume of 1870×10^6 m^3. The main subaqueous channel runs from the bay's 1.8 km wide entrance, with depths varying from 25 to 50 m up to 6 km inwards and along 24 km to the upper 20 km

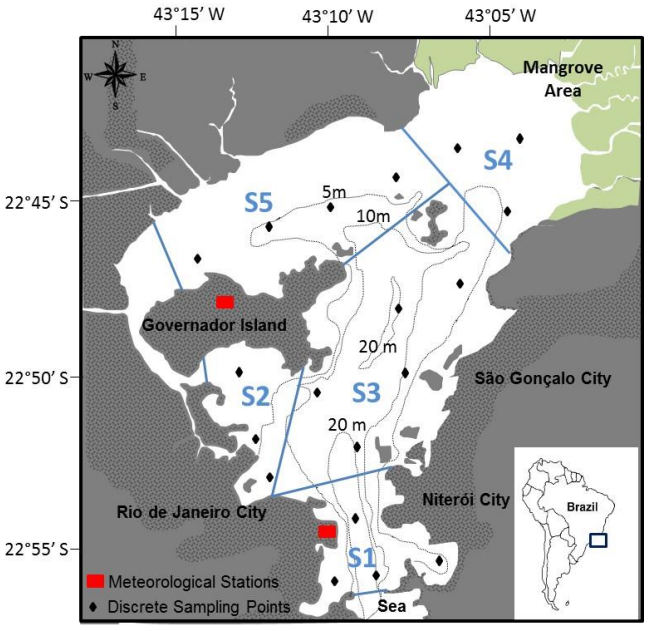

Figure 1. Map of Guanabara Bay. Dark grey indicates the urbanized areas. Green areas represent the mangrove localization. Black points represent the locations of the discrete sampling, black lines are isobaths, red squares represent the locations of the airports with the meteorological stations, and blue lines delimit the different sectors in the bay (S1 to S5).

wide bay, with depths down to about 2 to 3 m. The lateral portions of the bay feature small bays, with depths of about 2 m. It is a partially mixed estuarine embayment (Kjerfve et al., 1997), being completely mixed in wintertime but able to exhibit stratified conditions in summertime due to concomitant effects of sunlight (thermal stratification) and freshwater discharge (haline stratification), mostly in the central and inner regions (Bérgamo, 2010).

The bay is subject to a semi-diurnal microtidal regime, with an annual mean of 0.7 m and spring tides attaining 1.3 m. With the exception of the entrances of small rivers, salinities vary between 25 and 34. The time for renewal of 50 % of the total water volume is 11.4 days and water circulation is complex, as currents are modulated by tide and abrupt changes in the geomorphological configuration (Kjerfve et al., 1997). Circulation between the central and upper western regions is hampered by the presence of a large island (Governador Island, Fig. 1). At the bay's mouth, maximum water velocities vary between 0.8 and 1.5 m s^{-1} and seawater residence time is much shorter than in most inner regions, particularly behind Governador Island, where maximum current velocities are less than 0.3 m s^{-1} (Kjerfve et al., 1997).

Guanabara Bay is located in the intertropical zone, and its climate is subject to variability in both the annual temperature and precipitation regimes. The weather is tropical and humid (Bidone and Lacerda, 2004), with a warm and wet summer in October–March, and a drier winter in April–September. The most frequent winds in the bay from the north and northeast in spring and summer, with monthly average velocity of 5 m s^{-1}. Winds from the south and southeast are associated with polar cold weather fronts, which are more common in autumn and winter (Amarante et al., 2002).

The drainage basin has an area of 4080 km^2 and includes 35 small rivers and streams, 6 of which flow into the upper region of the bay and contribute up to 85 % of the total runoff to the bay. The average annual freshwater water discharge to the bay is 100 ± 59 m^3 s^{-1} and ranges from around 40 m^3 s^{-1} in winter to 190 m^3 s^{-1} in summer. Annual freshwater discharge is 9 times smaller than the bay's volume, which also contributes to the two-layered gravitational circulation (the ebb–flood oscillatory tidal current), resulting in the predominant saline (i.e. polyhaline) character of the waters (Kjerfve et al., 1997).

More than 7 million inhabitants discharge 25 m^3 s^{-1} of untreated domestic wastewaters into the bay (Kjerfve et al., 1997; Bidone and Lacerda, 2004), which contributes to a load of about 465 t day^{-1} of organic matter (FEEMA, 1998). Small channels directly connected to sewage outlets are completely anoxic, but these represent less than 5 % of the surface area of the bay. More intense cultural eutrophication since the 1950s (Borges et al., 2009) has also contributed to hypoxic conditions of bottom waters in some of the more confined lateral and upper regions of the bay (Paranhos et al., 1998; Ribeiro and Kjerfve, 2002). Fluxes of phosphorus are currently 9 times higher than those estimated since the late 1800s (Borges et al., 2009). According to Godoy et al. (1998), sedimentation rates have increased up to 14 times over the last 50 years, in parallel with a 10-fold increase in the flux of organic matter to the sediments (Carreira et al., 2002).

In this study, five sectors were defined for the treatment, computations and interpretation of the data (Fig. 1). Sector one (S1) corresponds to the region up to 3 km inwards from the narrow and deeper tidal channel, is characterized by a maximum of seawater exchange and material dispersion, and is partially mixed. Sector two (S2), located towards the western part of the bay, is delimited to the north by Governador Island, which creates a barrier for direct tidal advection of waters into the upper northwestern area of the bay. It is one of the most contaminated areas of Guanabara Bay. Sector three (S3) corresponds to the deeper channel which connects S1 (i.e. the bay's outlet to the South Atlantic) with the upper region. Sector four (S4), in the upper northeastern part of the bay, is shallow, moderately impacted and bordered by 90 km^2 of mangrove forest and non-urbanized land. Sector five (S5) is the most confined area of the bay, located to the northwest and behind Governador Island. It is shallow, has the longest residence time of waters, and also receives significant amounts of sewage waters. The small western channel connecting S2 and S5 was disregarded in our analysis, due to its difficult access and extreme degree of contamination. However, it covers less than 10 % of the entire sampled area.

2.2 Sampling strategy

Nine sampling campaigns were performed with a frequency varying between 30 and 45 days from April 2013 to April 2014. Each campaign consisted in continuous measurements of the partial pressure of CO_2 (pCO_2), salinity, temperature, Chl *a*, DO, pH and GPS position, all at a frequency of 1 min. Subsurface ($\sim$ 30cm) water was pumped alongside the boat. In addition to the spatial screening, the diurnal variations in water pCO_2 were estimated on four occasions within the upper and most eutrophic sectors (S4 and S5), and also once in S1, by performing lateral trajectories back and forth across the sectors from dawn (04:30) to afternoon or dusk (at the latest until 21:30). Diurnal measurements were made in August 2013 and January 2014, February and April 2014 (S4 and S5), and April 2014 (S1).

In addition, discrete sampling was performed at 16 to 19 stations along the continuous tracks (Fig. 1), except in December 2013, when only 8 stations could be sampled due to logistical problems. Water samples were collected in subsurface waters at $\sim$ 30 cm depth with a Niskin bottle, and then conditioned (i.e. fixed and/or kept on ice in the dark) for further chemical analysis in the laboratory. Vertical profiles of temperature, salinity, fluorescence and DO were performed at all discrete stations with an YSI 6600 V2 multiparameter probe.

2.3 Analytical procedures

2.3.1 Discrete parameters

Total alkalinity (TA) was determined on 10 mL of filtrate from GF/F filtered samples, using the classical Gran (1952) electro-titration method with an automated titration system (Metler Toledo model T50). The reproducibility of TA was 4 µmol kg^{-1} ($n = 7$). Measurements were compared to certified reference material (CRM, provided by A. G. Dickson from Scripps Institution of Oceanography) and consistent at a maximum precision level of ± 7 µmol kg^{-1}. Dissolved inorganic nitrogen (ammonia, nitrite, and nitrate) and phosphate were quantified as in Grasshof et al. (1999) and Chl *a* as in Strickland and Parsons (1972). Whatman GF/F filters were used for the Chl *a* analyses and the filtrate for the nutrient analyses. All water samples were kept in the dark and on ice during transport to their respective laboratories and nutrient samples and Chl *a* filters were kept at $-18\,^{\circ}$C in a freezer prior to analyses.

2.3.2 Online parameters

Continuous measurements of temperature, salinity, fluorescence and DO were performed with a calibrated YSI 6600 V2 multiparameter probe inserted in a flow-through customized acrylic chamber. The values of the fluorescence sensor were correlated with the discrete analysis of Chl *a* to derive a conversion factor. pH was measured continuously with a WTW 3310 pH meter equipped with a Sentix 41 electrode, which was also inserted in the chamber, and calibrated with a three-point standard (pH 4.01, pH 7.00 and pH 10.01) according to the National Institute of Standards and Technology (NIST) before each sampling campaign. The precision of the pH measurements was about 0.01 (after seven verifications against standards). As we have overdetermined the carbonate system (pCO_2, pH, and TA), we have chosen to use direct pCO_2 measurements and TA to calculate DIC. The pH measurements only served for a quality check. pCO_2 was measured using one marble-type equilibrator, through which seawater flowed (1–2 L min^{-1}) from the top to the bottom of the cylinder filled with marbles and air was pumped upwards (1 L min^{-1}) (Frankignoulle et al., 2001; Abril et al., 2006). The air in the equilibrator was dried before passing to a non-dispersive infrared gas analyser (LI-COR®, type LI-820). We used three gas mixture standards (pCO_2 of 410, 1007 and 5035 ppmv) to calibrate the LI-820 before each sampling (White Martins Certified Material, RJ, Brazil). We used N_2 passing through fresh soda lime to set the zero, and we used the standard at 1007 ppmv to set the span. We used the 410 and 5035 ppmv standards to check for linearity. Around seven verifications were performed after each calibration. The LI-820 signal was stable and linear in the range of calibration and observations in the field (0–5000 ppmv). We also verified the drift before and after each sampling campaign. The partial pressure of atmospheric CO_2 was measured in dry air twice a day, at the start and the end of the continuous runs. The precision and the accuracy of the pCO_2 measurements were about 3 and 5 ppmv, respectively.

Solar radiation, wind velocity (U10), accumulated precipitation and atmospheric temperature were recorded in the meteorological stations of Santos Dumont and Galeão airports (red squares in Fig. 1) and were provided by the Brazilian Institute of Aerial Space Control (ICEA). The data sets of solar radiation (Rs) were converted into daily-averaged photosynthetically active radiation (PAR) using a conversion factor PAR / Rs of 0.5 (Monteith, 1977).

2.3.3 Calculations

The carbonate system

Dissolved inorganic carbon (DIC) was calculated using two different pairs of measured parameters: pCO_2-TA and pH-TA using the carbonic acid constants sets proposed by Mehrbach et al. (1973) refitted by Dickson and Millero (1987), the borate acidity constant from Lee et al. (2010), and the CO_2 solubility coefficient of Weiss (1974). Calculations were performed in the CO2calc 1.2.9 program (Robbins et al., 2010). Both calculations gave very consistent DIC concentrations at ± 6.5 µmol kg^{-1}. DIC calculated from pCO_2–TA and pH–TA pairs gave an excellent agreement (slope: 1.008; $R^2 = 0.995$). The slope was not statistically different from 1 ($p = 0.20$) and the intercept was

not significantly different from 0 ($p = 0.86$). The excess of DIC (E-DIC, µmol kg^{-1}) was calculated as the difference between the in situ DIC (DIC in situ, µmol kg^{-1}) and a theoretical DIC at atmospheric equilibrium (DIC equilibrium, µmol kg^{-1}) according to Abril et al. (2003). The DIC equilibrium was calculated from observed TA and the atmospheric pCO_2 measured in the bay. The apparent oxygen utilization (AOU, µmol kg^{-1}) was calculated from the temperature, salinity and DO concentrations measured continuously with the probe and the theoretical DO saturation (Benson and Krause, 1984).

Diffusive air–sea CO_2 fluxes were computed from pCO_2 measured in the water and the atmosphere and a gas transfer velocity derived from wind and other physical drivers. We used the k wind parameterizations of Raymond and Cole (2001) and Abril et al. (2009), which are gas exchange coefficients specific for estuarine waters. The Raymond and Cole (2001) (RC01) equation is based on the compilation of gas transfer velocities derived from tracers applied to nine rivers and estuaries, using only wind speed as an entry parameter. The Abril et al. (2009) (A09) relationship is based on chamber flux measurements in seven estuaries, and uses wind speed, estuarine surface area, and water current velocity as entry parameters. We also calculated the fluxes with the parameterization of Wanninkhof (1992) (W92), which was initially developed for open ocean waters. The gas transfer coefficients normalized to a Schmidt number of 600 obtained with the three parameterizations were then converted to the gas transfer velocity of CO_2 at in situ temperature and salinity following the procedure of Jähne et al. (1987). Fluxes were computed for each sector of Guanabara Bay, using water pCO_2 representative for diurnal and seasonal variations.

The net community production (NCP)

The NCP was calculated by the changes in dissolved inorganic carbon (DIC) obtained from a set of lateral trajectories performed back and forth from dawn to dusk. As such, sampling addressed different times of the day at similar locations and NCP was computed from the diurnal DIC variations according to the following equation:

$$\mathrm{NCP} = ((\mathrm{DIC}_1 - \mathrm{DIC}_2)\rho d)/\Delta t - \mathrm{FCO}_2, \quad (1)$$

where NCP is in mmol m^{-2} h^1, DIC_1 and DIC_2 represent the salinity-normalized concentration of dissolved inorganic carbon (mmol kg^{-1}) during two consecutive trajectories (from dawn to dusk), ρ is the seawater density (kg m^{-3}), d is the average depth (m) of the area, t represents the time interval (hours) and FCO_2 is the carbon dioxide flux (mmol m^{-2} h^{-1}) across the water–atmosphere interface. The computations were carried out with the mean values of DIC during each trajectory.

Temperature and biological effect on pCO_2 variations

The temperature vs. biological effect on pCO_2 variations in Guanabara Bay was verified using the Takahashi et al. (2002) approach. The relative importance of the temperature and biological effects can be expressed as a ratio between both the temperature and the biology effect. The biological component is estimated by the seasonal amplitude of the temperature-normalized pCO_2 and the temperature component is characterized by the seasonal amplitude of the annual mean pCO_2 corrected for the seasonal temperature variation. The following equations were applied (Takahashi et al., 2002):

$$pCO_2 \text{ at } T_{\mathrm{mean}} = pCO_{2\mathrm{obs}} \times \exp[0.0423(T_{\mathrm{mean}} - T_{\mathrm{obs}})] \text{ (variations driven by biological effect)}, \quad (2)$$

$$pCO_2 \text{ at } T_{\mathrm{obs}} = pCO_{2\mathrm{mean}} \times \exp[0.0423(T_{\mathrm{obs}} - T_{\mathrm{mean}})] \text{ (variations driven by thermodynamic effect)}; \quad (3)$$

where T is the temperature in °C, and the subscripts "mean" and "obs" indicate the annual average and observed values, respectively. These equations were applied to summer and winter conditions as a whole. The biologic effect on the surface water, pCO_2 value, (ΔpCO_2)Bio, is represented by the seasonal amplitude of pCO_2 values corrected by the mean annual temperature, (pCO_2 at T_{mean}), using Eq. (1):

$$(\Delta pCO_2)\mathrm{Bio} = (pCO_2 \text{ at } T_{\mathrm{mean}})_{\max} - (pCO_2 \text{ at } T_{\mathrm{mean}})_{\min}, \quad (4)$$

where the subscripts "max" and "min" indicate the seasonal maximum and minimum values. The effect of temperature changes on the mean annual pCO_2 value, (ΔpCO_2)temp, is represented by the seasonal amplitude of (pCO_2 at T_{obs}) values computed using Eq. (2):

$$(\Delta pCO_2)\ \mathrm{Temp} = (pCO_2 \text{ at } T_{\mathrm{obs}})_{\max} - (pCO_2 \text{ at } T_{\mathrm{obs}})_{\min}. \quad (5)$$

A ratio of (ΔpCO_2)Temp/(ΔpCO_2)Bio (Temp/Bio) > 1 indicates dominance of the temperature effect over mean annual pCO_2 values, whereas a ratio < 1 indicates dominance of a biological effect (Takahashi et al., 2002).

2.4 Statistical analysis

A normality test was carried out by means of the Shapiro–Wilk test. If the data showed parametric distribution, we used a t test to compare averages. If the data showed non-parametric distribution, we used the Mann–Whitney test. The calculations of correlations between variables were performed with the Spearman rank coefficient. Simple linear regressions were calculated to compare calculated and measured variables (DIC and pH), and the comparison between slopes was made with one test equivalent to an analysis of

covariance (ANCOVA). For the principal component analysis (PCA) calculation, the sampling campaigns were taken as cases, and the parameters were taken as variables. The PCA technique starts with a correlation matrix presenting the dispersion of the original variables (data were normalized by z scores with average data for each sampling campaign), utilized for extracting the eigenvalues and eigenvectors. Thereafter, the principal components were obtained by multiplying an eigenvector by the original correlated variables. All statistical analyses were based on $\alpha = 0.05$. We utilized the STATISTICA 7.0 program to perform all PCA steps and the GraphPad Prism 6 program to perform the other statistical tests.

3 Results

3.1 Climatic, hydrological and biogeochemical conditions

Climatic conditions during the study period followed a classical seasonal trend (Fig. 2), with the exception of January 2014 and February 2014, when the air temperature was warmer (2.2 °C higher, $p < 0.001$, t test) than the average reference period of 60 years (1951–2010). The other sampled months had air temperature and precipitation consistent with historical data (Fig. 2), despite some deviations from the historical average, especially for accumulated precipitation. Sector-averaged surface water temperature in Guanabara Bay (Table 1) varied between 23.8 and 26.8 °C and salinity varied between 27.0 and 32.2. In the upper portion of the bay (S4 and S5), salinity decreased in winter and temperature increased in summer, with an observed maximum of 33.9 °C. S1, at the entrance of the bay, exhibited lowest temperatures and highest salinities, with little seasonal variation. A maximum seasonal amplitude of 3.4 and 2.8 °C of sector-averaged temperature occurred in S4 and S5, respectively. When considering sector-averaged values, seasonal contrasts were less than 2 salinity units in all sectors. Spatially, the most confined northern sectors, which receive more river water, showed the lowest salinity, particularly in the vicinity of river mouths, and during the rainy season, with a minimum of 14.6 in April 2013 in S4.

Average values for pH, TA, DIC, Chl *a* and nutrient data reported for each sector in Table 1 reflect the eutrophic (S1 and S3) to hypertrophic (S2, S4 and S5) conditions prevailing in Guanabara Bay, consistent with previous works (Rebello et al., 1988; Ribeiro and Kjerve, 2001). All water quality parameters (nutrients and Chl *a*) exhibited a large standard deviation (SD) to the mean. Ammonium (NH_4-N) was the dominant form of dissolved inorganic nitrogen (DIN) and reached average concentrations of around 45 and 27 µM in S2 and S5 and 8, 9 and 5 µM in S1, S3 and S4, respectively. The maximum range was recorded in S5 (0.13–130 µM NH_4-N) and the minimum range in the lower parts of S1 (8.15–22.5 µM NH_4-N).

Extremely high Chl *a* values were associated with high pH and moderate to low nutrient concentrations, indicating that nutrients were fixed into phytoplankton biomass. Average Chl *a* concentrations followed the trophic state gradient, increasing from the mouth of the bay toward its upper portion and also in the lateral embayments (Table 1). All sectors showed high spatial and temporal variability in Chl *a*. In general, highest values were recorded during summer conditions and lower values during winter. This feature has also been observed in other studies (Guenther et al., 2008; Guenther et al., 2012). S3, S4 and S5 experienced the densest phytoplankton blooms, with Chl *a* reaching maxima on one occasion of 537 µg L^{-1} in S3, 289 µg L^{-1} in S4 and 822 µg L^{-1} in S5.

3.2 Vertical structure of the water column

The vertical profiles for temperature, salinity, DO and Chl *a* in S1, S3 and S5, shown in Fig. 3, are well representative of other observations in the outer, middle and inner regions of Guanabara Bay, both for summer and winter conditions. During winter, the water column was well mixed in all sectors. Indeed, temperature and salinity showed few vertical variations during this season (Fig. 3a, c and e). Chl *a* and oxygen profiles were also vertically homogeneous, except in the most confined and shallow S5, where Chl *a* was typically 2.5 times higher in the first 2 m compared to the bottom (Fig. 3f). During summer, all sectors showed important thermal and saline stratification (Fig. 3g, i and k), halocline and thermocline being located almost at the same depth. In 20 m deep water columns (S1 and S3; Fig. 3g and i), an ∼ 4 m deep surface layer was ∼ 2–3°C warmer and had salinity ∼ 1–2 units lower than the bottom layer; in 5 m deep water column (S5; Fig. 3k), the warmer surface layer was ∼ 2 m deep with similar temperature and salinity contrasts between the surface and the bottom. The vertical water profile was also analysed to investigate the diurnal variations in temperature and salinity (Fig. 3k and l). Comparison between daytime and night-time conditions revealed that stratification was subject to diurnal variations, driven by temperature convection concomitant with a moderate mixing of water currents by microtidal action. Summer stratification of the water column was accompanied by a consistent vertical distribution of Chl *a* and oxygen, with a maximum in the surface layers and a minimum at the bottom. Note that the salinity varied less than the temperature over the day (> 2°C of variation in 5 h; Fig. 3k). Stratification apparently favoured phytoplankton development, as Chl *a* concentrations were highest (up to 240 µg L^{-1}) at the surface of the stratified water columns. These physical conditions were largely predominant in summer and in the shallowest, calmest and most confined sectors of the bay (S4 and S5).

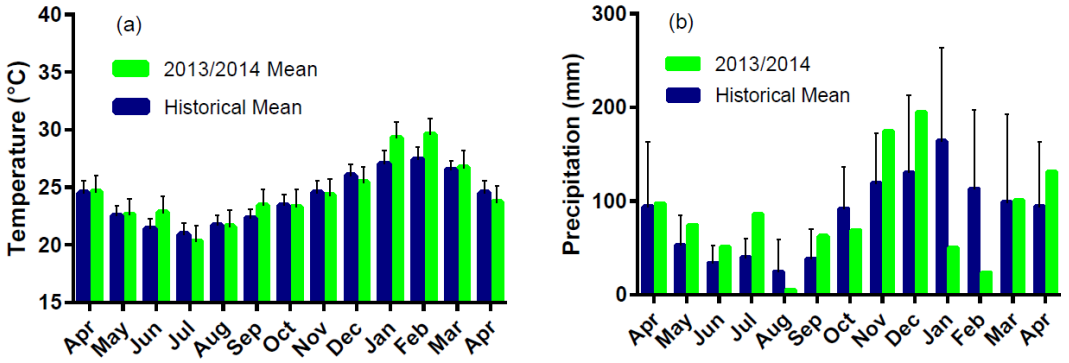

Figure 2. Meteorological conditions during the sampling period (in green) compared with historical values (1951–2014, in blue). **(a)** Presents the monthly accumulated precipitation; **(b)** presents the monthly average of atmospheric temperature.

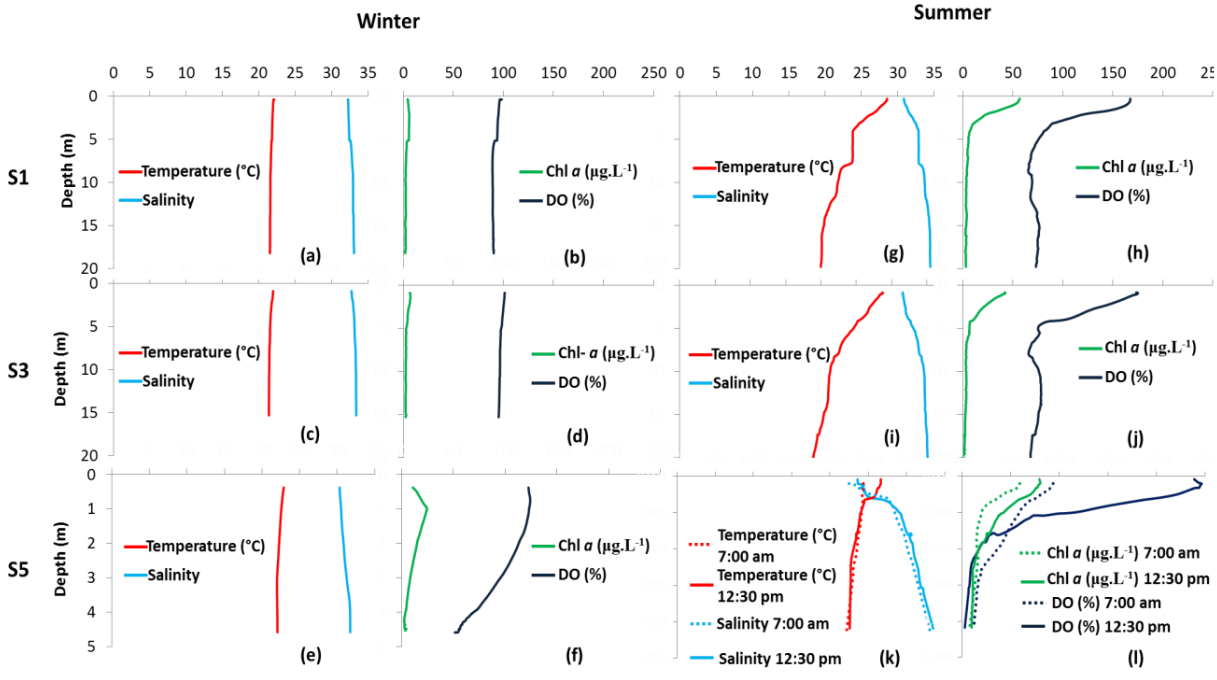

Figure 3. Typical vertical profiles of salinity, temperature, dissolved oxygen (DO) and chlorophyll *a* (Chl *a*) in the water column. Profiles are shown for S1, S3 and S5 in summer and winter conditions. Note the different depth scale for the S5. The dotted line in **(k)** and **(l)** shows the night-time profile (07:00), whereas the full line shows a daytime profile (12:30) for the same day at the same station.

3.3 Spatial distributions of pCO_2 in surface waters

Spatial distributions of surface water pCO_2 measured continuously along the trajectories revealed strong spatial gradients between and/or inside each sector, from over- to undersaturation with respect to the atmosphere (Fig. 4). Temporally and spatially, water pCO_2 was inversely correlated with dissolved oxygen ($R^2 = -0.88$; $n = 9002$; $p < 0.0001$) and Chl *a* ($R^2 = -0.54$; $n = 9004$; $p < 0.0001$). S1 presented pCO_2 values close to the atmospheric equilibrium, with moderate temporal variation around this average (411 ± 145 ppmv). DO and Chl *a* in S1 were 103 ± 29 % and $19 \pm 22\ \mu g\ L^{-1}$, respectively. S2, close to most urbanized area, showed highest heterogeneity, from a maximum pCO_2 value of 3750 ppmv in hypoxic waters (DO = 2 % saturation) at the vicinity of the highly polluted urban channels in January 2014 (Fig. 4g) to strong undersaturation, as low as 50 ppmv, related to a bloom formation (Chl $a = 212\ \mu g\ L^{-1}$) in January 2014. In S2, the extent of pCO_2 supersaturation apparently induced by the urban sewage loads was favoured by strong rains the day before sampling and lower PAR incidence in July, August and September 2013 compared to all the other cruises (Fig. 4). In S3, S4 and S5, which account for 75 % of the surface sampled area of Guanabara Bay, pCO_2 was predominantly below the atmospheric equilibrium, particularly during daytime summer cruises (Fig. 4

Table 1. Mean (± standard deviation), minimum, maximum and number of observations (N) of the principal physicochemical properties of the waters of Guanabara Bay for the sampling period, separated by sector. DL: detection limit.

	Sector 1	Sector 2	Sector 3	Sector 4	Sector 5
Temp. (°C)	23.8 ± 1.7 (21.0–29.3) $N = 1918$	25.5 ± 2.2 (22.1–32.4) $N = 1047$	25.4 ± 2.1 (22.1–31.5) $N = 2035$	26.8 ± 2.6 (22.0–32.3) $N = 1594$	26.7 ± 2.2 (22.6–33.9) $N = 2397$
Sal.	32.2 ± 2.1 (25.4–34.9) $N = 1918$	30.3 ± 2.4 (17.7–33.7) $N = 1047$	29.8 ± 3.0 (15.1–33.8) $N = 2035$	27.0 ± 4.3 (14.6–33.2) $N = 1594$	27.2 ± 3.5 (16.6–32.9) $N = 2397$
DO (%)	103 ± 29 (48–221) $N = 1918$	97 ± 59 (2–263) $N = 1047$	138 ± 51 (56–357) $N = 2035$	142 ± 62 (30–361) $N = 1594$	160 ± 69 (46–370) $N = 2397$
pCO_2 (ppmv)	411 ± 145 (104–747) $N = 1918$	711 ± 561 (50–3715) $N = 1046$	286 ± 157 (41–660) $N = 2035$	307 ± 256 (29–2222) $N = 1594$	272 ± 293 (22–2203) $N = 2397$
pH (NBS)	8.20 ± 0.16 (7.90–8.71) $N = 1581$	8.15 ± 0.32 (7.33–8.96) $N = 910$	8.35 ± 0.23 (7.88–8.96) $N = 1790$	8.34 ± 0.29 (7.39–9.01) $N = 1490$	8.44 ± 0.31 (7.51–9.23) $N = 2225$
TA ($\mu mol\,kg^{-1}$)	2240 ± 92 (1942–2320) $N = 44$	2291 ± 99 (1890–2488) $N = 32$	2168 ± 177 (1507–2500) $N = 40$	2045 ± 369 (2111–3920) $N = 39$	2137 ± 166 (1479–2314) $N = 53$
DIC ($\mu mol\,kg^{-1}$)	1979 ± 112 (1713–2120) $N = 44$	2037 ± 258 (1520–2513) $N = 32$	1841 ± 250 (1328–2286) $N = 32$	1652 ± 254 (1088–2111) $N = 35$	1752 ± 256 (1193–2186) $N = 52$
Chl a ($\mu g\,L^{-1}$)	19.1 ± 22.0 (2.0–128.0) $N = 34$	46.2 ± 51.4 (3.3–212.9) $N = 33$	57.6 ± 90.0 (1.6–537.2) $N = 33$	69.2 ± 60.2 (13.1–288.8) $N = 32$	107.7 ± 101.8 (1.5–822.1) $N = 47$
NO_3-N (µM)	3.50 ± 3.30 (0.13–12.50) $N = 34$	3.72 ± 4.93 (< DL −18.63) $N = 33$	4.12 ± 5.27 (0.16–19.12) $N = 32$	2.14 ± 3.29 (< DL −14.74) $N = 33$	1.92 ± 2.08 (0.04–9.20) $N = 47$
NO_2-N (µM)	1.60 ± 1.92 (0.05–7.30) $N = 36$	2.59 ± 2.89 (0.10–10.67) $N = 33$	1.81 ± 2.58 (< DL −10.79) $N = 33$	1.46 ± 2.74 (0.03–9.37) $N = 33$	1.71 ± 1.98 (0.03–7.08) $N = 47$
NH_4-N (µM)	8.15 ± 6.26 (0.09–22.50) $N = 37$	44.9 ± 25.2 (0.15–94.73) $N = 33$	9.10 ± 9.48 (0.04–37.95) $N = 33$	4.96 ± 6.92 (0.04–29.29) $N = 33$	26.82 ± 27.67 (0.13–130.12) $N = 47$
PO_4-P (µM)	1.11 ± 0.60 (0.11–2.44) $N = 37$	5.28 ± 3.88 (0.17–20.79) $N = 33$	1.51 ± 1.07 (0.17–1.10) $N = 33$	1.10 ± 0.79 (0.03–2.96) $N = 33$	2.23 ± 2.17 (0.02–8.72) $N = 47$

and Table 1). Massive phytoplankton blooms were sampled during our survey, characterized by extreme patchiness in summer. For example, an extreme of 22 ppmv pCO_2, 350 % saturated DO and 550 $\mu g\,L^{-1}$ Chl a was recorded in February 2014 in a brown/red bloom. In S3, S4 and S5, water pCO_2 was lower than 150 ppmv around midday in all seasons. These blooms and the associated pCO_2 undersaturation occurred in S4 and S5 during winter and progressively spread to the entire bay during the summer months (Fig. 4). From September 2013 to February 2014, midday undersaturation was encountered over the whole bay, except for the urban-impacted S2 (Fig. 4). Finally, some increases in water pCO_2 above the atmospheric equilibrium (up to a maximum of 2200 ppmv) were observed in July 2013, August 2013 and April 2014, in the northeastern parts of S4 and S5, related to river plumes. Before reaching the bay waters of S4, these riverine plumes flowed across a preserved mangrove area. However, the extent of these small plumes was limited

(Fig. 4) and their contribution to the sector CO_2 balance was apparently negligible.

3.4 pCO_2 diurnal variations

The five back-and-forth tracks revealed important diurnal changes in water pCO_2 in S4 and S5, but not in S1 (Fig. 5). In the S1 in February 2014 (Fig. 5d), night-time (predawn) pCO_2 (451 ± 38 ppmv) was not significantly different ($p > 0.05$ Mann–Whitney test) from daytime pCO_2 (466 ± 26 ppmv). In contrast, in S4 and S5, rapid and significant decreases in water pCO_2 were recorded in the early hours of the morning, followed by a relatively stable undersaturation from 10:00 and all throughout the afternoon (Fig. 5). For instance, in September 2014, pCO_2 decreased from 800 ppmv at 08:30 to 200 ppmv at 13:40 at the same geographical location (Fig. 5a). The decrease in water pCO_2 occurred relatively quickly on all occasions at around 09:30, which apparently corresponded to the hour of maximum photosynthetic activity by phytoplankton. Thus, 09:30 was used as the limit to separate night-time pCO_2 from daytime pCO_2. In S4 and S5, pCO_2 changes from night-time to daytime were from 591 ± 231 to 194 ± 114 ppmv in September 2013, from 163 ± 40 to 116 ± 25 ppmv in January 2014, from 346 ± 166 to 146 ± 106 ppmv in February 2014, and from 637 ± 421 to 265 ± 186 ppmv in April 2014. In all these cases, water pCO_2 was significantly higher ($p < 0.001$; Mann–Whitney test) before than after 09:30. Consequently, S4 and S5 shifted from a CO_2 source at night-time to a CO_2 sink during daytime in September 2013 and April 2014, but remained a CO_2 sink throughout the entire day and night in January and February 2014. In addition to these five back-and-forth tracks described in Fig. 5, we could compare water pCO_2 values measured on the same day in the early morning (before 09:30) with those measured in late afternoon in S1, S3 and S4. Consequently, our data provided a fairly good indication of the diurnal variability in pCO_2 throughout the entire sampling period, in all sectors except for S2 (Fig. 6).

3.5 Seasonal variations

Clear seasonal changes were observed in pCO_2 of surface waters (Fig. 6), with higher values in winter (April 2013, July 2013, August 2013, September 2013 and April 2014) than in summer (October 2013, December 2013, January 2014 and February 2014). Seasonal variations in DO and Chl *a* mirrored the pCO_2 variations, with a maximum phytoplanktonic biomass and oxygen saturation in summer, when pCO_2 was at its minimum. S1 was a source of atmospheric CO_2 during winter (pCO_2 of 501 ± 98 ppmv) but a sink during summer (pCO_2 of 304 ± 117 ppmv). S2 presented the highest pCO_2 differences between winter (923 ± 484 ppmv) and summer (423 ± 530 ppmv), with high standard deviations resulting from spatial heterogeneity for both periods (Fig. 4). In S3, S4 and S5, CO_2 undersaturation prevailed along the year, except in winter and during night-time, when oversaturations prevailed. In these three sectors, oxygen remained oversaturated throughout the year. Average measured values of pCO_2 for winter and summer were respectively 353 ± 141 and 194 ± 127 in S3, 380 ± 286 and 203 ± 159 in S4, and 364 ± 343 and 132 ± 74 ppmv in S5. Note that these averages are in their majority based on daytime measurements and that integrated yearly average CO_2 fluxes had to be quantified by accounting for both seasonal and diurnal variations (see following section and discussion).

3.6 Gas transfer velocities, CO_2 fluxes at the air–sea interface and NCP

Wind speeds (12 h averaged) varied between 1.4 and 3.9 m s^{-1}, were significantly higher during summer than winter ($p < 0.001$; *t* test), and were significantly higher during daytime than night-time ($p < 0.001$; *t* test) (Table 2). Instantaneous wind speed showed some peaks at a maximum of 15 m s^{-1} during short (< 1 h) events. Wind speeds measured at the meteorological station in the southern part of the bay were higher (S1, S2 and S3) than those recorded at the station in the northern region (S4 and S5) (Table 2).

Calculated gas transfer velocities averaged over daytime and night-time periods varied between 0.8 and 12.3 cm h^{-1} (Table 2). k_{600} values calculated from the equation of Abril et al. (2009) that accounts for the wind velocity, the fetch effect linked to estuarine size and the current velocity were systematically higher than those calculated from the relationships of Raymond and Cole (2001) and Wanninkhof (1992), which consist in exponential functions of wind velocity, with the former being specific for estuarine waters and the latter primarily developed for open ocean waters. Average k_{600} values based on 15 min wind speed were not significantly different from k_{600} based on 12 h average wind speed, showing that short storms had a negligible impact on daily-integrated gas transfer velocities. CO_2 fluxes were calculated using the measured pCO_2 in each sector during the respective period: summer and winter, daytime and night-time. In the absence of data, we interpolated pCO_2 from surrounding areas and/or measurement periods. For S2, the only sector that was not sampled at night, we applied the mean diurnal variations in S1 and S3. Because of the relatively narrow range of k_{600} variation, calculated CO_2 fluxes followed the pattern of surface water pCO_2 and varied between 14.6 mmol m^{-2} h^{-1} in the polluted S2 during winter and night-time and -9.7 mmol m^{-2} h^{-1} in dense phytoplanktonic blooms of S5 during summer and daytime (Table 2). Time-integrated CO_2 fluxes, accounting for seasonal and daily variations, revealed that all sectors except S2 behaved as CO_2 sinks on an annual basis.

The NCP estimates for Guanabara Bay encompassed four sampling campaigns (September 2013, January 2014, February 2014 and April 2014). The values ranged between 51 and 255 mmol m^{-2} d^{-1}, with an annual average of

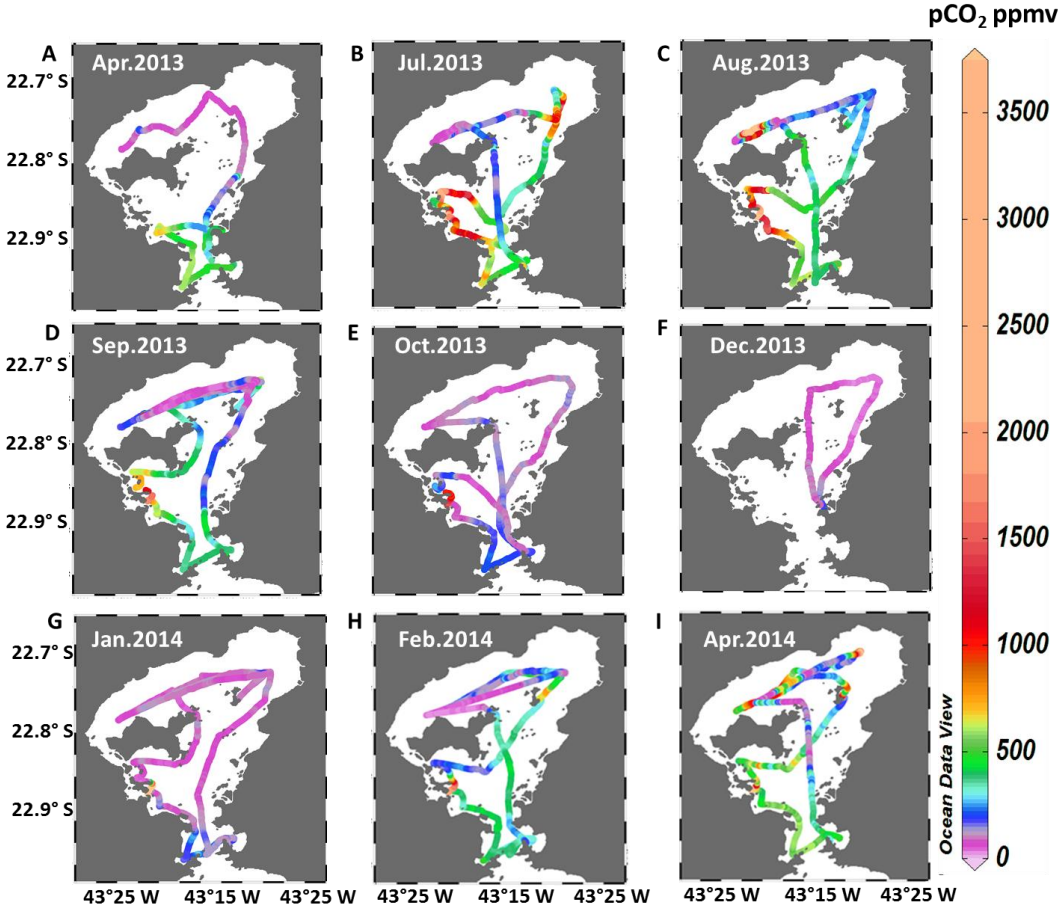

Figure 4. Concentration maps of continuous pCO_2 measurements in surface waters of Guanabara Bay for all the sampling campaigns.

$143 \pm 56\,\mathrm{mmol\,m^{-2}\,d^{-1}}$. The summertime period presented an average of $161 \pm 49\,\mathrm{mmol\,m^{-2}\,d^{-1}}$, whereas for wintertime the NCP was $126 \pm 51\,\mathrm{mmol\,m^{-2}\,d^{-1}}$. All values of NCP were positive, indicating that the upper sectors of Guanabara Bay were autotrophic.

4 Discussion

4.1 Estuarine typology: comparing Guanabara Bay with other estuaries

The results of the continuous measurements and the concomitant discrete sampling of water quality parameters showed that, in terms of CO_2 atmospheric exchange, Guanabara Bay does not follow the patterns of a typical drowned-river-valley estuary with a marked longitudinal estuarine gradient between its fresh and marine water endmember sources (Pritchard, 1952). Rather, Guanabara Bay corresponds to a tropical marine-dominated system, owing to the small freshwater discharge relative to its water volume and tidal exchange, maintaining 85 % of the bay with salinities always higher than 25. Its geomorphological characteristics and rather complex circulation of water masses make it difficult to apply standard approaches to discern sources or sinks from composite plots between salinity and material concentrations (Bourton and Liss, 1976). Furthermore, Guanabara Bay has been considered one of the world's most degraded embayments, characterized by constant eutrophic to hypertrophic conditions and the frequent occurrence of red tides (Rebello et al., 1988; Villac and Tennenbaum, 2010; Guenther et al., 2012).

The CO_2 behaviour in Guanabara Bay is different from that in most of documented estuaries worldwide. Indeed, the majority of studies that were conducted in macrotidal, turbid and river-dominated estuaries reveal that these systems are heterotrophic and emit large amounts of CO_2 both in temperate and tropical regions (Frankignoulle et al., 1998; Borges and Abril, 2011; Sarma et al., 2012). These drowned-valley, river-dominated estuaries also exhibited a significant inverse trend between salinity and pCO_2 (Frankignoulle et al., 1998), which was not observed in Guanabara Bay. The absence of a negative relationship between pCO_2 and salinity for the range of 27 to 32 is in fact more consistent with observations in some estuarine plumes (although less pro-

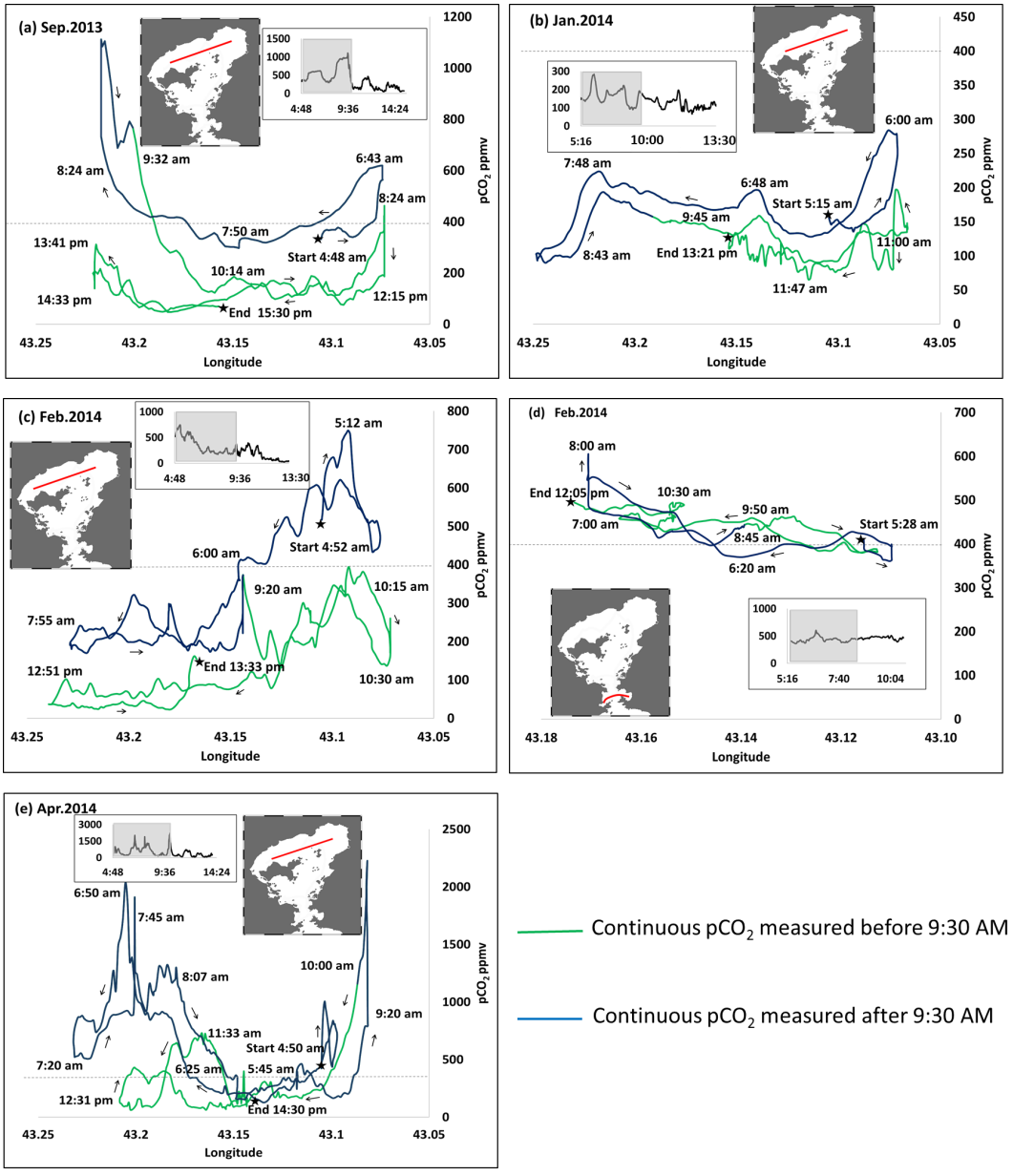

Figure 5. Diurnal variations in pCO_2 concentrations. The ship back-and-forth tracks are indicated as red lines in small maps. Arrows show the boat direction, and sampling times are indicated along each track. Blue parts of the tracks are considered as night-time (< 09:30) and green parts as daytime (> 09:30). Inserted small graphs also show the water pCO_2 evolution vs. time, and the shaded area represents the sampling before 09:30 (night-time). The grey lines indicate the atmospheric pCO_2 (400 ppmv). Note the different pCO_2 scales for each survey.

nounced), where pCO_2 undersaturation and diurnal variations are often reported (Borges and Frankignoulle, 1999; Borges and Frankignoulle, 2002; Dai et al., 2009; Bozec et al., 2011). Therefore, our results in Guanabara Bay are still consistent with the comparative analysis of CO_2 dynamics in river- and marine-dominated estuaries by Jiang et al. (2008). In Guanabara Bay, salinities lower than 27 were confined to the upper region at the mouths of the small rivers in S4 (max. $pCO_2 =$ 2222 ppmv), S5 (max. $pCO_2 = 2203$ ppmv) and some polluted channels of S2 (max. $pCO_2 = 3715$ ppmv) (Table 1 and Fig. 4). However, these heterotrophic and strong CO_2 degassing regions are relatively small when compared to the total surface area. In contrast, pCO_2 in S1, which is directly affected by marine water intrusion, exhibited minor diurnal and seasonal variations fluctuating around the atmospheric value of 400 ppmv. However, S3, S4 and S5 as a whole, which cover around 75 % of the bay's area, behaved as a net CO_2 sink on an annual basis, with concen-

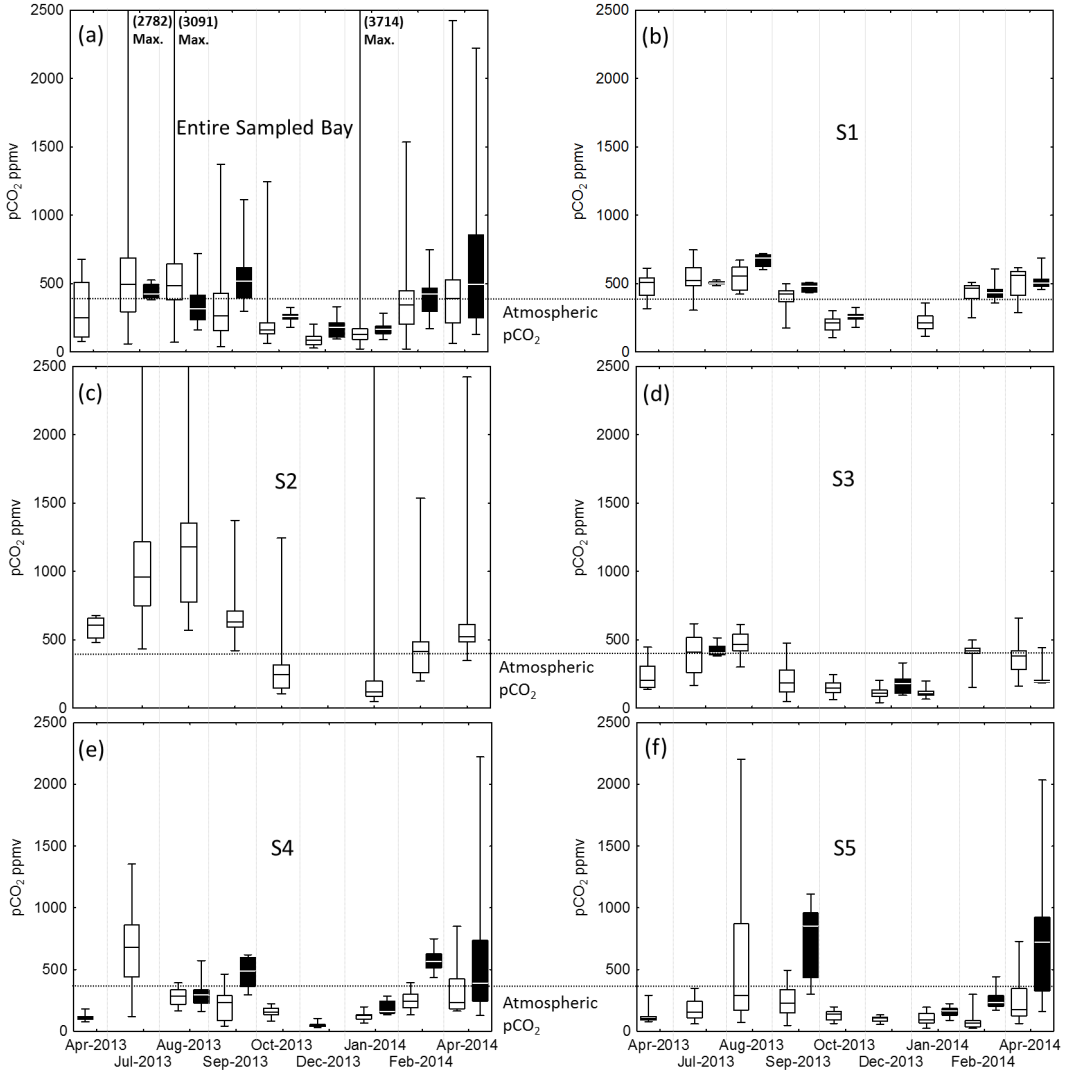

Figure 6. Box plots (maximum, 75th percentile, median, 25th percentile and minimum) of pCO_2 data for all the campaigns **(a)** and for each individual sector (**b**, **c**, **d**, **e** and **f**). Black box plots represents the night-time data (< 09:30), when available, and white box plots represent daytime data (> 09:30).

trations even down to about 30 ppmv on some occasions (Table 2). These three sectors are subject to weaker tidal currents, higher water residence times, and stratification at shallow depths, favouring CO_2 uptake by phytoplankton primary production and autotrophic metabolism, especially during summer. Indeed, thermal or haline stratification of estuarine waters has been identified as a determinant factor that favours the ecosystem to act as a CO_2 sink (Borges 2005; Chou et al., 2013). Low pCO_2 values in surface waters were reported for the inner shelf of the Changjiang Estuary (Chou et al., 2013), the outer Loire estuary (Bozec et al., 2012), the lower Pearl River estuary (Dai et al., 2008), the Amazon River plume (Körtzinger, 2003) and on the Mississippi River-dominated continental shelf (Huang et al., 2015), all with enhancement of stratification stimulating phytoplankton bloom development and uptake of CO_2. Low pCO_2 values were also observed in estuaries which receive low freshwater discharge and present low water exchange with the sea (Jiang et al., 2008; Koné et al., 2009; Maher and Eyre, 2012; Sarma et al., 2012).

The comparison of the E-DIC versus AOU values (Fig. 7) from our study with a compilation of data obtained for 24 estuaries, in mostly river-dominated estuaries located in temperate regions (Borges and Abril, 2011), illustrates the specific metabolic characteristics of Guanabara Bay. The negative E-DIC and AOU values found for Guanabara Bay suggest the system is autotrophic. The 1 : 1 line represents the quotient between CO_2 and O_2 during planktonic primary production and community respiration (Borges and Abril 2011). The values close along this line for Guanabara Bay

Table 2. Summary of calculated mean values for wind speed (U_{10}), gas exchange coefficient (k_{600}) and CO_2 fluxes at the air–sea interface in each sector and the whole of Guanabara Bay. Diurnal variations (night-time < 09:30; daytime > 09:30), seasonal means (winter and summer) and time-integrated values are reported. W92 is the data calculated according to k_{600} of Wanninkhof (1992), RC01 is the data calculated according to k_{600} of Raymond and Cole (2001), and A09 is data calculated according to k_{600} of Abril et al. (2009).

			U_{10} ($m\,s^{-1}$)	k_{600} ($cm\,h^{-1}$)			CO_2 flux ($mmol\,m^{-2}\,h^{-1}$)		
				W92	RC01	A09	W92	RC01	A09
Sector 1	Winter	Night-time	1.8	1.2	3.5	7.2	0.55	1.59	3.37
(47 km^2)		Daytime	2.5	2.6	4.7	9.0	0.50	1.19	2.33
	Summer	Night-time	2.5	2.7	4.8	9.2	−0.84	−1.27	−2.35
		Daytime	3.8	6.6	8.5	12.3	−1.23	−3.88	−5.42
	Time-integrated		2.6	3.2	5.3	9.4	−0.25	−0.57	−0.51
Sector 2	Winter	Night-time	1.9	1.9	3.7	7.5	5.19	7.74	14.61
(32 km^2)		Daytime	2.4	2.3	4.4	8.8	3.29	4.99	10.29
	Summer	Night-time	2.5	3.1	4.8	9.2	1.75	1.97	2.87
		Daytime	3.3	4.4	6.2	10.9	1.12	1.28	2.02
	Time-integrated		2.5	2.9	4.7	9.1	2.27	4.00	7.44
Sector 3	Winter	Night-time	1.4	0.8	3.0	6.1	−0.13	0.06	0.34
(96 km^2)		Daytime	2.6	2.8	4.9	9.2	−0.19	−0.79	−1.53
	Summer	Night-time	2.8	3.0	5.0	9.7	−1.97	−3.28	−6.37
		Daytime	3.9	6.7	8.4	12.2	−4.82	−6.22	−9.65
	Time-integrated		2.6	3.3	5.3	9.3	−1.77	−2.56	−4.29
Sector 4	Winter	Night-time	1.5	0.9	3.2	6.2	−0.10	−0.33	−0.59
(55 km^2)		Daytime	2.3	2.3	4.4	7.8	−1.04	−1.26	−2.00
	Summer	Night-time	2.1	1.7	4.0	7.4	−0.24	−0.43	−0.76
		Daytime	3.2	4.6	6.4	9.9	−4.28	−5.90	−9.13
	Time-integrated		2.2	2.3	4.5	7.8	−1.41	−1.97	−3.12
Sector 5	Winter	Night-time	1.5	0.9	3.2	6.1	0.83	3.32	5.88
(80 km^2)		Daytime	2.4	2.4	4.5	8.0	−1.61	−2.67	−4.87
	Summer	Night-time	2.1	1.8	4.0	7.4	−2.67	−3.25	−4.99
		Daytime	3.1	4.2	6.0	9.6	−4.27	−6.21	−9.73
	Time-integrated		2.2	2.3	4.4	7.7	−1.93	−2.20	−3.42
All bay	Winter	Night-time					0.78	1.86	3.53
(310 km^2)		Daytime					−0.24	−0.46	−0.67
	Summer	Night-time					−1.29	−1.92	−3.45
		Daytime					−3.42	−5.02	−7.73
	Time-integrated						−1.10	−1.38	−2.07

suggest that gross primary production and total (autotrophic and heterotrophic) respiration are coupled, and largely dominated the signal, with a strong biological control on the production/consumption of these gases. Many data from other estuaries are situated well above the 1 : 1 line, especially at high pCO_2 values, indicating lateral inputs of dissolved CO_2 from tidal marshes or mangroves, faster equilibration of oxygen with the atmosphere than carbon dioxide due to differences in solubility and the buffering capacity of the carbonate system, and/or anoxic respiration in sediments (Cai et al., 1999; Abril et al., 2002; Bouillon et al., 2008; Borges and Abril, 2011). In Guanabara Bay, the extent of mangrove forests is not great, and the volume of water exchanged with the mangrove sediments is moderate due to the modest tidal amplitude. For that reason, we could not find supersaturated pCO_2 conditions near the mangrove region, at least at about 2 km distance from the mangrove. This suggests that dissolved CO_2 export from the mangrove is low and probably associated with a rapid consumption of mangrove-derived DIC by the phytoplankton.

4.2 Meteorological and biological control of pCO_2 in Guanabara Bay

A PCA was performed to better identify the variable contributions of the data. For each sampling day, we calculated the mean values of pCO_2, DO, pH, Chl *a*, temperature, salinity, wind velocity, PAR incidence and also the 7 days of

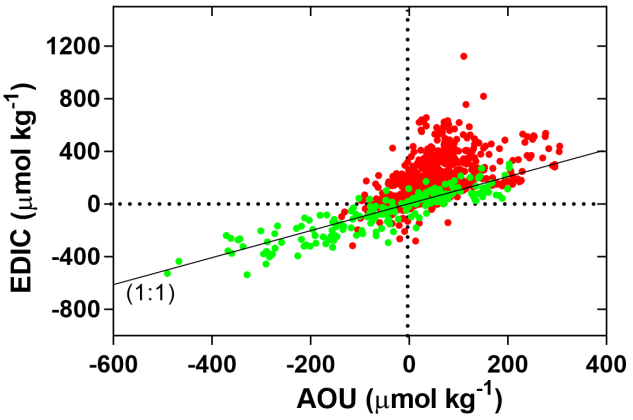

Figure 7. Relationship between the excess dissolved inorganic carbon (E-DIC) and apparent utilization of oxygen (AOU) in Guanabara Bay (green dots) compared to those reported in 24 estuarine environments (red dots; Borges and Abril, 2011). The 1 : 1 line represents the quotient between CO_2 and O_2 during the processes of photosynthesis and respiration.

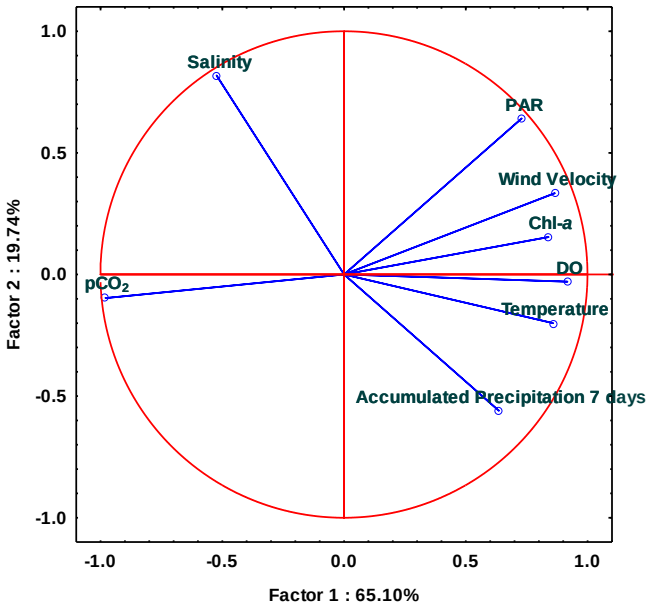

Figure 8. Principal components analysis (PCA) based on mean values for each sampling campaign of the physical and biogeochemical properties of the water (temperature, salinity, pCO_2, DO and Chl *a*) and meteorological conditions (wind velocity and accumulated precipitation of 7 days before each survey). The data set was normalized by *z* scores.

accumulated precipitation. The PCA revealed a strong meteorological control on the pCO_2 dynamics in Guanabara Bay (Fig. 8). Factor 1 explains 65 % of the total variance, revealing that pCO_2 was well separated and negatively related to DO, Chl *a*, temperature, wind velocity and PAR incidence. This suggests a strong external meteorological control on phytoplankton dynamics and, in turn, the CO_2, DO and Chl *a* at spatial and temporal scales. Indeed, the high incident light simultaneously provides energy for phytoplankton growth and favours the development of thermal stratification, particularly in the shallow and less hydrodynamic regions (Fig. 3). In the tropics, high light incidence combined with the presence of nutrients contributes to phytoplankton blooms and CO_2 depletion both directly, by supplying light for photosynthesis, and indirectly, by favouring stratification of the water column. It is worth noting that high wind speed in the region of Guanabara was correlated with high PAR and, consequently, gas exchange was favoured during daytime, when CO_2 depletion attained its maximum. In contrast, salinity and the 7-day accumulated precipitation were not related to the other parameters, and dominated the factor 2 of the PCA, which explains about 19 % of the variance in the data. This suggests that pulsated inputs of freshwater, typical of tropical storms, affect salinity in Guanabara Bay but have little impact on the intensity of blooms and the CO_2 uptake by the phytoplankton.

Our diurnal measurements along the hypertrophic S4 and S5 also showed marked differences in pCO_2 concentrations between daytime and night-time. The night-time pCO_2 values were about 30 % higher than daytime (differing by up to 395 ppmv). As the PAR incidence increased throughout the day, the surface pCO_2 decreased due to the enhancement of photosynthesis and rapid formation of thermal stratification (Figs. 3 and 5). Our report of strong diurnal variation in pCO_2 in Guanabara Bay (Fig. 5) reveals how photosynthesis and respiration processes vary temporally, especially in areas with high phytoplankton biomass (indicated by Chl *a* values above 50, sometimes reaching 200 μg L^{-1}). In their study of primary production based on oxygen incubations in Guanabara Bay, Rebello et al. (1988) postulated that some intriguing very low rates in Chl *a*-rich samples were due to the occurrence of CO_2 limitation. Indeed, the extremely low values of pCO_2 observed in S5 (for example 24 ppm or 0.6 μmol kg^{-1} of dissolved CO_2) confirm that CO_2 might be one of the limiting factors for primary production. However, in such CO_2-limiting conditions, phytoplankton would need to take up bicarbonate using the proton pump mechanism and the carbonic anhydrase enzyme (Kirk, 2011). Some diurnal variations in pCO_2 controlled by biological activity have been reported in several other estuarine systems worldwide (Dai et al., 2009; Bozec et al., 2011; Yates et al., 2007; Zhang et al., 2013). In the Bay of Brest, a temperate coastal embayment, the phytoplankton blooms were responsible for 10 to 60 % of the seasonal pCO_2 drawdown observed during spring, equivalent to 100–200 ppmv (Bozec et al., 2011). In Tampa Bay, a shallow subtropical estuary, the diurnal variations in pCO_2 (median of 218 ppmv) were largely influenced by primary productivity and respiration of benthic communities (Yates et al., 2007). Also, Zhang et al. (2013) reported diurnal pCO_2 variations mainly controlled by biological ac-

tivities (maximum 218 ppm in autumn) in a Chinese tropical open bay dominated by fringing reefs; however, calcification was also an important driver of diurnal pCO_2 variations in winter. In one suite of different coastal ecosystems in the South China Sea, including inshore and onshore locations, Dai et al. (2009) concluded that temperature was a major driver of pCO_2 diurnal variability in the oligotrophic and offshore regions (10–16 ppmv variations), tidal effects in the nearshore (41–152 ppmv), and biological metabolism in the coral reef system (up to 608 ppmv diurnal variations). Thus, it is clear that diurnal variations must be accounted for in estuarine CO_2 budget assertions. Otherwise, budget estimates based on daytime pCO_2 measurements only might shift the conclusions towards an overestimate of the CO_2 sink, or an underestimate of the CO_2 source. Therefore, we use pCO_2 measurements at different hours of the day and night in order to integrate the diurnal variations.

The contributions of temperature and biological activity for Guanabara Bay were estimated at 33 and 255 ppmv, respectively, showing the strong influence of biological productivity upon pCO_2 dynamics in this tropical coastal embayment (ratio of 0.12). Some authors utilized the same approach in other estuarine systems with different dominances between temperature and the biological effect (Bozec et al., 2011; Zhang et al., 2012; Hunt et al., 2014). The temperature dominating effect was detected for Jiaozhou Bay (Yellow Sea); Zhang et al. (2012) obtained pCO_2 variation differences of 93 and 78 ppmv for temperature and biological activity, respectively (weak temperature prevalence and ratio of 1.19). In the Kennebec Estuary (USA), Hunt et al. (2014) found different rations according to the salinity zones and showed that, in general, higher ratios prevailed at low salinities (1.9–2.1), with higher temperature control on pCO_2 variations. Bozec et al. (2011), on the other hand, in one interannual approach, encountered a mean value of 0.49 in the Bay of Brest, a temperate embayment in France, confirming that the biological processes were the main driver of the seasonal pCO_2 dynamic. The ratio for Guanabara Bay is much lower than in all these systems, and also consistent with atypical CO_2 dynamics.

4.3 Eutrophication and CO_2 dynamics

In several coastal systems worldwide, important CO_2 changes, either increasing or decreasing, have been attributed to eutrophication processes (Gypens et al., 2009; Borges and Gypens, 2010; Cai et al., 2011; Sunda and Cai, 2012; Chou et al., 2013). Eutrophication occurs when massive anthropogenic inputs of both organic (mainly domestic) and inorganic (agricultural or industrial) nutrients (sometimes over several decades) enrich estuarine waters and sediments with bioavailable nitrogen and phosphorus (Rabalais et al., 2009). Increases in pCO_2 have been reported in river-dominated estuaries at the vicinity of megacities (Frankignoulle et al., 1998; Zhai et al., 2007; Sarma et al., 2012). When sewage is discharged in such river-dominated systems, heterotrophy is enhanced and CO_2 outgassing increases (Zhai et al., 2007; Sarma et al., 2012). Indeed, environmental conditions in these turbid estuarine waters strongly limit primary production in favour of heterotrophy. Turbidity, together with stratification, is indeed a key parameter that explains pCO_2 variation in estuaries (Jiang et al., 2008; Borges and Abril 2011). In Guanabara Bay, sewage also predominates as a source of organic nutrients (Bidone and Lacerda, 2004). However, the pCO_2 spatial distribution (Fig. 4) suggests that mineralization of this domestic organic matter occurs predominantly within the sewage network itself and in small rivers and channels and their plumes that represent a small surface area in the bay. It can be noted, for example, that pCO_2 oversaturation was more extended in S2 in August 2013, which corresponds to a sampling just after strong rains over the city of Rio de Janeiro. Mineralization of organic matter in these extremely polluted areas leads to rapid CO_2 (and probably CH_4) outgassing and, concomitantly, contributes to a long-term enrichment of the bay in bioavailable nitrogen and phosphorus (Paranhos et al., 1998; Ribeiro and Kjerfve, 2002).

Except for these peripheral zones, most sectors of Guanabara Bay experienced massive algal blooms due to the optimal conditions for primary production, including nutrient, light, and water column stratification. The driving phytoplankton assemblages of Guanabara Bay are typical for eutrophic to hypertrophic systems that are largely dominated by bloom and also red tide forming nanoplankton, filamentous cyanobacteria and some microplankton (Valentin et al., 1999; Santos et al., 2007; Villac and Tennenbaum, 2010). Preliminary investigations of the collected material from this study suggests that cyanobacteria were frequently encountered in S2, S4 and S5 during the nine sampling periods, and a great deal of patchiness was observed with a succession of intense red-, brown- and/or green-coloured waters, leading to the marked short spatial variability in pCO_2, DO and Chl *a*. In the waters dominated by phytoplankton blooms, the pCO_2 values were always extremely low and the sink characteristics were prevalent, with high CO_2 uptake and autotrophy characteristics. It has been shown that, during summer, the heterotrophic bacterial production (BP) lay within the range of only 0.4–19 % of primary production (PP) at the surface and 5–52 % at the bottom, being nutrient-dependent (Guenther et al., 2008). Our spatial and temporal pCO_2 data set (Fig. 4) also suggests that the most confined part of the inner bay apparently behaved as a "bloom genesis region" that can spread phytoplanktonic production, biomass, and associate CO_2 consumption over the rest of the estuarine system. Indeed, CO_2-depleted waters were confined to S4 and S5 in October 2013 and progressively extended to all sectors (except S2) in January 2014. During this period, conditions became ideal for bloom developments with increasing air and water temperature and the development of water stratification (Figs. 4 and 6).

Eutrophication thus enhances the low surface pCO_2 concentrations in Guanabara Bay. Phytoplankton use more nutrients and dissolved CO_2 in the surface waters and produce larger biomass of organic matter. When this additional material reaches the bottom, the organic matter and associated nutrients are recycled, increasing pCO_2 and decreasing the oxygenation of bottom waters (Fig. 3k, l). Some authors have recently discussed the increase in bottom water acidification enhanced by coastal eutrophication, especially in stratified ecosystems (Cai et al., 2011; Sunda and Cai, 2012). It has been shown that water column stratification and bottom water stagnation enhance the isolation of O_2 and CO_2 in deeper waters and, consequently, their exchange between bottom and surface waters (Chen et al., 2007). Koné et al. (2009) reported a consistent CO_2 vertical distribution in the Aby and Tendo lagoons, in Ivory Coast, where a warmer, fresher, Chl *a*-rich surface layer was depleted in CO_2 and nutrients, whereas a more saline and anoxic bottom layer was enriched in CO_2 and nutrients. Gypens et al. (2009) developed and validated a process-based model in the Scheldt estuary plume, which revealed that eutrophication could make the system shift from a net source of atmospheric CO_2 to a net sink if anthropogenic nutrient loads increased, thereby stimulating the carbon fixation by autotrophs. Chou et al. (2013) also suggested that a human-induced increase in nutrient loading may have stimulated primary production and thus enhanced the CO_2 uptake capacity on the inner shelf off the Changjiang Estuary. Our results reveal that the impact of eutrophication on estuarine systems in terms of CO_2 exchange strongly depends on their typology. Drowned-valley, river-dominated, "funnel-type" estuaries, which are generally light-limited and heterotrophic, respond in a completely way to estuarine plumes, marine-dominated lagoons or embayments like Guanabara Bay, where optimal conditions for autotrophic primary production occur over large surface areas. These estuarine types are different in their hydrological and geomorphological configuration, availability of light, diversity of primary producer and heterotrophic assemblages, and their response to increasing nutrient loading (Smith et al., 2010; Cloern et al., 2014). Depending on the hydrodynamics, the additional organic carbon produced by enhanced eutrophication can be buried, mineralized, and/or exported. In quiescent embayments like Guanabara Bay, long-term burial can be significant (Carreira et al., 2002), resulting in a net uptake and storage of atmospheric carbon within the ecosystem.

4.4 Air–water CO_2 fluxes in Guanabara Bay

The spatial and temporal CO_2 fluxes were integrated for the bay, taking into account the diurnal and seasonal variations in pCO_2, wind speed, and gas exchange coefficients. Efforts were made to sample all the sectors of the bay with different PAR intensities (higher, medium and low intensity, for each sampling day, and especially in the more eutrophic waters). Characteristic daytime and night-time pCO_2 values were deduced from the five back-and-forth observations in S4 and S5, and from the comparison of early morning (before 09:30) pCO_2 data with late afternoon data in S1, S3 and S4. Compared to seasonal changes, diurnal changes were significant, surface pCO_2 sometimes shifted from sink behaviour in the evening to source behaviour at the end of the night, or sometimes remained undersaturated throughout the entire night (Fig. 6). Except for S2, the more polluted sector, and the only one acting as a CO_2 source, our data could be used to integrate diurnal variability in pCO_2 throughout the sampling period (Fig. 6). For S2, the only region that was not sampled during the night, the values of the diurnal differences obtained in S1 and S3 were applied, which seems reasonable owing to their similar Chl *a* concentrations.

From comparison of the three k_{600} used for the calculated fluxes, the k_{600} of Abril et al. (2009) can be considered the higher flux estimate, based on chamber measurements in nine estuarine systems, whereas the k_{600} of Wanninkhof (1992) provides a more conservative value. The model of Raymond and Cole (2001), based on non-intrusive "tracers-only" data, provided intermediate fluxes compared to the other two models. k_{600} values varied from 0.8 to 12.3 cm h^{-1}, which corresponds to wind speed velocities between 1.8 and 3.9 m s^{-1}. Current velocity (a few dozen centimetres per second) contributed to a minor fraction of k_{600} in the Abril et al. (2009) equation. On an annual basis, Guanabara Bay was a net sink of atmospheric CO_2 (year-integrated flux of −9.6, −12.0 and −18.1 mol C m^2 yr^{-1} for k_{W02}, k_{RC01} and k_{A09}, respectively) but with strong differences at temporal and spatial scales. On a daily basis, summer CO_2 uptake was maximal in S3, S4 and S5, with daily fluxes of −190, −110 and −170 mmol C m^2 d^{-1}, respectively, whereas in the winter fluxes decreased to −14, −30 and +12 mmol C m^2 d^{-1}, respectively (note that S5 changed from a large sink in summer to a slight source in winter). S1 was a moderate source in winter (+60 mmol C m^2 d^{-1}) and a moderate sink in summer (−90 mmol C m^2 d^{-1}), as well as on an annual basis (−4.45 mol C m^2 yr^{-1}). In the highly polluted S2, where a large part of the domestic organic matter is apparently respired, a strong annual outgassing occurred (+213 mmol C m^2 d^{-1}). However, this region occupies only about 10 % of the surface-sampled area of the bay. It is interesting to note that the winds were stronger during the midday/afternoon periods than during the night/early morning periods. This conforms to the classical daily wind cycle at coastal regions guided by the thermal difference between the land and the water surface (Amarante et al., 2002), which apparently favours the CO_2 sink. Higher wind speed during daytime and in summer also favoured the CO_2 uptake.

The sink of CO_2 at air–sea interface showed values very close to the burial rates of organic carbon in the sediments. Table 3 presents one summary of the documented carbon fluxes in the Guanabara Bay. Carreira et al. (2002) found a 10-fold increase in the flux of organic carbon to the sediments in the last 50 years (maximum of 114 mmol C m^{-2} d^{-1}

Table 3. Summary of the documented carbon fluxes in the Guanabara Bay.

Inputs	mmol C m^{-2} d^{-1}	Comment
CO_2 air–water flux	26–49[a]	All bay average; this study
CO_2 air–water flux	33–102[a]	Sectors 3, 4 and 5; this study
Organic carbon load from sewage	43	All bay average; FEEMA (1998); most organic carbon seems to be mineralized in sewage network
River DIC, DOC and TOC inputs	Undocumented	
Internal processes	**mmol C m^{-2} d^{-1}**	**Comment**
NCP	51–225 (143)[b]	Sectors 4 and 5; this study
NPP	60–300 (170)[b]	Sectors 2, 3 and 5; Rebello et al. (1988)
Total respiration	Undocumented	
Outputs	**mmol C m^{-2} d^{-1}**	**Comment**
Organic carbon burial	27–114	Sectors 3, 4 and 5; Carreira et al. (2002); Monteiro et al. (2011)
DIC and TOC export to the coastal area	Undocumented	

[a] Annual average according to the k_{600} model parameterizations of Wanninkhof (1992) and Abril et al. (2009). The lower value refers to the model of Wanninkhof (1992), whereas the higher value refers to the model of Abril et al. (2009). [b] Range and annual average in parentheses.

in S5). Our annual budget of carbon uptake at the air–water interface was 105 mmol C m^2 d^{-1} for this same region, showing that Guanabara Bay is, in fact, a strong CO_2 sink and has an autotrophic metabolism. The autotrophic nature of Guanabara Bay is also confirmed by the relationship between autotrophic and heterotrophic communities (Guenther and Valentin, 2008; Guenther et al., 2008). Rebello et al. (1988) estimated phytoplankton primary production rates from monthly measurements over an annual cycle to vary between 60 and 300 mmol C m^{-2} d^{-1}, with highest rates in the lateral and upper regions of the bay. The bacterial production used only a small fraction of the dissolved organic carbon pool, which had a turnover between 23 and 71 days in waters of the bay (Guenther et al., 2008). Average net primary production (NPP) was 170 mmol C m^{-2} d^{-1}. Compared with our results, the NPP values are very close to those found for the carbon uptake at air–water interface for summer conditions in S3, S4 and S5, being 200, 149 and 189 mmol C m^{-2} d^{-1}, respectively. After normalization to the total surface area of Guanabara Bay, the total average organic load from sewage and rivers is about 43 mmol OrgC m^2 d^{-1} (FEEMA, 1998), compared to the annual CO_2 uptake at the air–water interface of 49 mmol C m^2 d^{-1}. However, the pCO_2 spatial distribution supports the idea that most of the sewage-derived organic carbon is respired at the vicinity of the urban area, and little contributes to the carbon budget in the rest of the bay, except for S2. In addition, molecular and isotopic characterization of the particulate organic matter of Guanabara Bay revealed the predominance of autochthonous organic matter (Kalas et al., 2009). What also leads us to the conclusion that Guanabara Bay behaves as a net autotrophic system are the high positive values of NCP in S4 and S5. The annual average NCP was 143 mmol m^{-2} d^{-1}, which is the highest value compared to the compiled data set of Borges and Abril (2011), which included 79 estuaries, of which 66 are net heterotrophic, 12 net autotrophic, and 1 balanced. The summertime period showed the highest values of NCP and coincides with the strongest sink of CO_2 at the air–water interface. Guanabara Bay showed NCP values near that found in the tropical eutrophic Bojorquez Lagoon (Mexico) at the annual scale (Reyes and Merino, 1991) and in the subtropical coastal waters of Hong Kong during summertime (Yuan et al., 2011), both systems being highly impacted by sewage discharge.

5 Conclusions

In Guanabara Bay, annual uptake of atmospheric CO_2 associated with a net burial of organic matter in sediments was due to the synergic and cumulative effects of three factors: (i) an estuarine typology of marine-dominated embayment with fairly long residence times of saline waters together with nutrient inputs in its upper sectors permitting phytoplanktonic developments, (ii) the tropical climatic conditions that increase light availability and favour the stratification of the water column, and (iii) a long-term discharge of untreated domestic waters that have enriched the bay in nutrients and led to eutrophication. Eutrophication has also modified the phytoplanktonic assemblages toward smaller, more produc-

tive and short-lived groups (Villac and Tennenbaum, 2010), including some nitrogen-fixing species (cyanobacteria). A net autotrophic metabolism of Guanabara Bay is attested by the annual CO_2 uptake at the air–water interface, the positive and high NCP values, the low bacterial production relative to the primary production (Guenther et al., 2008), and the large burial of autochthonous organic carbon to the sediments (Carreira et al., 2002). It is the first estuarine system where the synergy of these three factors has been clearly identified as the predominant driver of CO_2 dynamics and carbon balance. Some other cases of net CO_2 uptake have been reported in some relatively polluted tropical coastal lagoons in Ivory Coast (Koné et al., 2009), in three temperate and marine-dominated Australian estuaries (Maher and Eyre, 2012), in temperate and tropical estuarine plumes either preserved (Körtzinger, 2003) or human-impacted (Cai, 2003; Zhai and Dai, 2009; Bozec et al., 2012), and in some pristine Arctic and subarctic fjords (Rysgaard et al., 2012; Ruiz-Halpern et al., 2010). In contrast, inner and low-salinity regions of most river-dominated, drowned-valley, "funnel-type" estuaries, which are generally well-mixed and relatively turbid environments, have been documented as heterotrophic and CO_2 emitters under tropical (Araujo et al., 2014), temperate (Frankignoulle et al., 1998) and boreal (Silveneoieen et al., 2008) climates, regardless of the anthropogenic pressure (Abril et al., 2003, 2004; Zhai et al., 2007; Borges and Abril, 2011; Cai, 2011; Sarma et al., 2012).

Our findings of a net annual CO_2 sink in Guanabara Bay indicate that more field data are needed, in particular in the highly productive tropical coastal ocean, in order to adequately integrate estuarine CO_2 fluxes at the global scale. In Brazil, most previous studies have concerned river-dominated estuaries, especially along the northern and northeastern coast, which all behave as CO_2 sources (Souza et al., 2009; Araujo et al., 2014; Noriega and Araujo, 2014). In contrast to Guanabara Bay, highest CO_2 fluxes correspond to denser population in the watersheds of these net heterotrophic systems (Noriega et al., 2014). In fact, the Brazilian coast presents several estuarine types (river estuarine deltas, estuaries, lagoons and large embayments) which have very different metabolisms (Bernardes et al., 2012) but where CO_2 fluxes have as yet to established. Large pCO_2 temporal variations can be expected, for instance, in a phytoplankton-dominated coastal lagoon in Brazil that exhibited an annually balanced metabolism but with seasonal shifts between autotrophic and heterotrophic conditions (Carmouze et al., 1991; Knoppers et al., 1999a, b). Lagoons dominated by macroalgae or microphytobenthos exhibited different metabolic trends, but still with a significant potential for a net uptake of atmospheric CO_2 (Knoppers, 1994). Undersampling coastal embayments and lagoons with clear and stratified waters, compared to turbid and well-mixed, river-dominated estuaries, would potentially lead to an overestimation of the regional estuarine CO_2 budget. In addition, diurnal variations might impact the net CO_2 budget more significantly in autotrophic systems than in heterotrophic systems and need to be assessed in the field. Continuous pCO_2 measurements on autonomous buoys (e.g. Frankignoulle et al., 2003; Bozec et al., 2011) are very promising tools for reaching sufficient temporal resolution. We also showed that pCO_2 dynamics were strongly correlated with meteorological conditions. Taking into account the fact that the last projections of Intergovernmental Panel on Climate Change (IPCC) include unequivocal predictions of the climate system warming for the next years (Stocker et al., 2013), the increase in water temperature can reinforce the net sink of Guanabara Bay.

Acknowledgements. This research was funded by the Science Without Border programme of the Brazilian National Council of Research and Development (CNPq-PVE 401726/2012-6). This project supported G. Abril with a senior scientist grant, N. Brandini with a post-doc grant and LCCJr with a PhD grant for visiting EPOC. B. A. Knoppers is a senior scientist of CNPq (proc. no. 301572/2010-0). The meteorological data were kindly provided by the Brazilian Institute of Aerial Space Control (ICEA, Ministério da Defesa, Comando da Aeronáutica, Org. 2°SGT. BMT Antonio Carlos), and the global estuarine data by Alberto Borges (Liège University). We are grateful to Wei-Jun Cai and an anonymous referee for improving the quality of this manuscript through their valuable suggestions and recommendations.

Edited by: S. Bouillon

References

Abril, G., Nogueira, E., Hetcheber, H., Cabeçadas, G., Lemaire, E., and Brogueira, M.: Behaviour of organic carbon in nine contrasting European estuaries, Estuar. Coast. Shelf Sci., 54, 241–262, 2002.

Abril, G., Etcheber, H., Delille, B., Frankignoulle, M., and Borges, A.V.: Carbonate dissolution in the turbid and eutrophic Loire estuary, Mar. Ecol-Prog. Ser., 259, 129–138, 2003.

Abril G., Commarieu M., Maro D., Fontugne M., Guérin F., and Etcheber, H.: A massive dissolved inorganic carbon release at spring tide in a highly turbid estuary, Geophys. Res. Lett., 31, L09316, doi:10.1029/2004GL019714, 2004.

Abril, G., Richard, S., and Guérin, F.: In-situ measurements of dissolved gases (CH_4 and CO_2) in a wide range of concentrations in a tropical reservoir using an equilibrator, Sci. Total Environ, 354, 246–251, 2006.

Abril, G., Commarieu, M., Sottolichio, A., Bretel, P., and Guérin, F.: Turbidity limits gas exchange in a large macrotidal estuary, Estuar. Coast. Shelf Sci., 83, 342–348, 2009.

Allen, M. R., Frame, D. J., Huntingford, C., Jones, C., Lowe, J. A., Meinshausen, M., and Meinshausen, N.: Warming caused by cumulative carbon emissions towards the trillionth tonne, Nature, 458, 1163–1166, 2009.

Amarante, O. A., Silva, F. J., and Rios Filho, L. G.: Atlas Eólico, Estado do Rio de Janeiro, Secretaria de Estado da Energia, da Indústria Naval e do Petróleo, Rio de Janeiro, 64 pp.,

available at: http://www.cresesb.cepel.br/publicacoes/download/atlas_eolico/AtlasEolicoRJ.pdf, 2002.

Araujo, M., Noriega, C., and Lefèvre, N.: Nutrients and carbon fluxes in the estuaries of major rivers flowing into the tropical Atlantic, Front. Mar. Sci., 1, 1–16, 2014.

Bauer, J. E., Cai, W.J., Raymond, P., Bianchi, T. S., Hopkinson, C. S., and Regnier, P. G.: The changing carbon cycle of the coastal ocean, Nature, 504, 61–70, doi:10.1038/nature12857, 2013.

Benson, B. B. and Krause, D.: The concentration and isotopic fractionation of oxygen dissolved in freshwater and seawater in equilibrium with the atmosphere, Limnol. Oceanogr., 29, 620–632, 1984.

Bérgamo, A. S.: Caracteristicas hidrograficaz, da circulacao, e dos transportes de volume e sal na Baia de Guanabara (RJ): variacoes sazonais e moduladas pela mare, Ph.D. thesis, Universidade de Sao Paulo, Sao Paulo, 200 pp., 2010.

Bernardes, M. C., Knoppers, B. A., Rezende, C. E., Souza, W. F., and Ovalle, A. R.: Land-sea interface features of four estuaries on the South America Atlantic coast, Braz. J. Biol., 72, 761–774, 2012.

Bidone, E. D. and Lacerda, L. D.: The use of DPSIR framework to evaluate sustainability in coastal areas. Case study: Guanabara Bay basin, Rio de Janeiro, Brazil, Reg. Environ. Change, 4, 5–16, 2004.

Borges, A. C., Sanders, C. J., Santos, H. L. R., Araripe, D. R., Machado, W., and Patchineelam, S. R.: Eutrophication history of Guanabara Bay (SE Brazil) recorded by phosphorus flux to sediments from a degraded mangrove area, Mar. Pollut. Bull., 58, 1750–1754, 2009.

Borges, A. V.: Do we have enough pieces of the jigsaw to integrate CO_2 fluxes in the coastal ocean?, Estuaries, 28, 3–27, 2005.

Borges, A. V. and Abril, G.: Carbon Dioxide and Methane Dynamics in Estuaries, in: Treatise on Estuarine and Coastal Science, edited by: Eric, W. and Donald, M., Academic Press, Amsterdam, 119–161, 2011.

Borges, A. V. and Frankignoulle, M.: Daily and seasonal variations of the partial pressure of CO_2 in surface seawater along Belgian and southern Dutch coastal areas, J. Mar. Syst., 19, 251–266, 1999.

Borges, A. V. and Frankignoulle, M.: Distribution and air-water exchange of carbon dioxide in the Scheldt plume off the Belgian coast, Biogeochemistry, 59, 41–67, 2002.

Borges, A. V. and Gypens, N.: Carbonate chemistry in the coastal zone responds more strongly to eutrophication than ocean acidification, Limnol. Oceanogr., 55, 346–353, 2010.

Bouillon, S., Borges, A. V., Castañeda-Moya, E., Diele, K., Dittmar, T., Duke, N. C, Kristensen, E., Lee, S. Y., Marchand, C., Middelburg, J. J., Rivera-Monroy, V., Smith T. J., and Twilley, R. R.: Mangrove production and carbon sinks: a revision of global budget estimates, Global Biogeochem. Cy., 22, GB2013, doi:10.1029/2007GB003052, 2008.

Bourton, J. D. and Liss, P. S.: Estuarine Chemistry, Academic Press, London, 1976.

Bozec, Y., Merlivat, L., Baudoux, A. C., Beaumont, L., Blain, S., Bucciarelli, E., Danguy, T., Grossteffan, E., Guillot, A., Guillou, J., Répécaud, M., and Tréguer, P.: Diurnal to inter-annual dynamics of pCO_2 recorded by a CARIOCA sensor in a temperate coastal ecosystem (2003–2009), Mar. Chem., 126, 13–26, 2011.

Bozec, Y., Cariou, T., Macé, E., Morin, P., Thuillier, D., and Vernet, M.: Seasonal dynamics of air-sea CO_2 fluxes in the inner and outer Loire estuary (NW Europe), Estuar. Coast. Shelf Sci., 100, 58–71, 2012.

Bricker, S., Ferreira, J., and Simas, T.: An integrated methodology for assessment of estuarine trophic status, Ecol. Modell., 169, 39–60, 2003.

Cai, W.-J., Pomeroy, L. R., Moran, M. A., and Wang, Y. C.: Oxygen and carbon dioxide mass balance for the estuarine-intertidal marsh complex of five rivers in the southeastern US, Limnol. Oceanogr., 44, 639–649, 1999.

Cai, W.-J.: Riverine inorganic carbon flux and rate of biological uptake in the Mississippi River plume, Geophys. Res. Lett., 30, 1032, doi:10.1029/2002GL016312, 2003.

Cai, W.-J.: Estuarine and coastal ocean carbon paradox: CO_2 sinks or sites of terrestrial carbon incineration?, Annu. Rev. Mar. Sci., 3, 123–145, 2011.

Cai, W.-J., Hu, X., Huang, W.-J., Murrell, M. C., Lehrter, J. C., Lohrenz, S. E., Chou, W.-C., Zhai, W., Hollibaugh, J. T., and Wang, Y.: Acidification of subsurface coastal waters enhanced by eutrophication, Nat. Geosci., 4, 766–770, 2011.

Carmouze, J., Knoppers, B. A., and Vasconcelos, P. A.: Metabolism of Saquarema Lagoon, Brazil, Biogeochemistry, 2, 129–148, 1991.

Carreira, R. S., Wagener, A. L. R., Readman, J. W., Fileman, T. W., Macko, S. A., and Veiga, Á.: Changes in the sedimentary organic carbon pool of a fertilized tropical estuary, Guanabara Bay, Brazil: an elemental, isotopic and molecular marker approach, Mar. Chem., 79, 207–227, 2002.

Chen, C. C., Gong, G. C., and Shiah, F. K.: Hypoxia in the East China Sea: One of the largest coastal low oxygen areas in the world, Mar. Environ. Res., 64, 399–408, 2007.

Chen, C.-T. A., Huang, T.-H., Chen, Y.-C., Bai, Y., He, X., and Kang, Y.: Air–sea exchanges of CO_2 in the world's coastal seas, Biogeosciences, 10, 6509–6544, doi:10.5194/bg-10-6509-2013, 2013.

Chou, W.-C., Gong, G.-C., Cai, W.-J., and Tseng, C.-M.: Seasonality of CO_2 in coastal oceans altered by increasing anthropogenic nutrient delivery from large rivers: evidence from the Changjiang-East China Sea system, Biogeosciences, 10, 3889–3899, doi:10.5194/bg-10-3889-2013, 2013.

Cloern, J.: Our evolving conceptual model of the coastal eutrophication problem, Mar. Ecol. Prog. Ser., 210, 223–253, 2001.

Cloern, J. E., Foster, S. Q., and Kleckner, A. E.: Phytoplankton primary production in the world's estuarine-coastal ecosystems, Biogeosciences, 11, 2477–2501, doi:10.5194/bg-11-2477-2014, 2014.

Cohen, J. E., Small, C., Mellinger, A., Gallup, J., and Jeffrey S.: Estimates of coastal populations, Science, 278, 1209–1213, 1997.

Dai, M., Zhai, W., Cai, W.-J., Callahan, J., Huang, B., Shang, S., Huang, T., Li, X., Lu, Z., Chen, W., and Chen, Z.: Effects of an estuarine plume-associated bloom on the carbonate system in the lower reaches of the Pearl River estuary and the coastal zone of the northern South China Sea, Cont. Shelf Res, 28, 1416–1423, 2008.

Dai, M., Lu, Z., Zhai, W., Chen, B., Cao, Z., Zhou, K., Cai, W., and Chen, C. A.: Diurnal variations of surface seawater pCO_2 in contrasting coastal environments, Limnol. Oceanogr., 54, 735–745, 2009.

Dickson, A. G. and Millero, F. J.: A comparison of the equilibrium constants for the dissociation of carbonic acid in seawater media, Deep-Sea Res., 34, 1733–1743, 1987.

Doney, S. C., Fabry, V. J., Feely, R. A., and Kleypas, J. A.: Ocean Acidification: The Other CO_2 Problem, Ann. Rev. Mar. Sci., 1, 169–192, 2009.

FEEMA: Qualidade da agua da Baıa da Guanabara – 1990 a 1997, Secretaria de Estado de Meio Ambiente, Fundaçao Estadual de Engenharia do Meio Ambiente, Rio de Janeiro, 187 pp., 1998.

Frankignoulle, M., Abril, G., Borges, A., Bourge, I., Canon, C., Delille, B., Libert, E., and Theate, J. M.: Carbon Dioxide Emission from European Estuaries, Science, 282, 434–436, 1998.

Frankignoulle, M., Borges A., and Biondo R.: A new design of equilibrator to monitor carbon dioxide in highly dynamic and turbid environments, Water Res., 35, 344–347, 2001.

Frankignoulle, M., Biondo, R., Théate, J. M., and Borges, A. V.: Carbon dioxide daily variations and atmospheric fluxes over the Great Bahama Bank using a novel autonomous measuring system. Caribb. J. Sci., 39, 257–264, 2003.

Gattuso J. P., Frankignoulle, M., and Wollast, R.: Carbon and carbonate metabolism in coastal aquatic ecosystems, Annu. Rev. Ecol. Syst., 29, 405–434, 1998.

Godoy, J. M., Moreira, I., Bragan, M. J., Wanderley, C., and Mendes, L. B.: A study of Guanabara Bay sedimentation rates, J. Radioanal. Nucl. Ch., 227, 157–160, 1998.

Gran, G.: Determination of the equivalence point in potentiometric titrations-Part II, Analyst, 77, 661–671, 1952.

Grasshoff, K., Ehrhardt, M., and Kremling, K. (Eds.): Methods of Seawater Analysis, third ed., Wiley-VCH, Weinhein, 1999.

Guenther, M. and Valentin, J.L. Bacterial and phytoplankton production in two coastal systems influenced by distinct eutrophication processes, Oecolog. Brasiliensis, 12, 172–178, 2008.

Guenther, M., Paranhos, R., Rezende, C., Gonzalez-Rodriguez, E., and Valentin, J.: Dynamics of bacterial carbon metabolism at the entrance of a tropical eutrophic bay influenced by tidal oscillation, Aquat. Microb. Ecol., 50, 123–133, 2008.

Guenther, M., Lima, I., Mugrabe, G., Tenenbaum, D. R., Gonzalez-Rodriguez, E., and Valentin, J. L.: Small time scale plankton structure variations at the entrance of a tropical eutrophic bay (Guanabara Bay, Brazil), Braz. J. Oceanogr., 60, 405–414, 2012.

Guo, X., Cai, W.-J., Huang, W-J., Wang, Y., Chen, F., Murrell, M.C., Lohrenz, S. Dai, M., Jiang, L.-Q. and Culp, R.: CO_2 dynamics and community metabolism in the Mississippi River plume, Limnol. Oceanogr., 57, 1–17, 2012.

Gypens, N., Borges, A. V., and Lancelot, C.: Effect of eutrophication on air-sea CO_2 fluxes in the coastal Southern North Sea: a model study of the past 50 years, Glob. Chang. Biol., 15, 1040–1056, 2009.

Huang, W.-J., Cai, W.-J., Wang, Y., Lohrenz, S. E., and Murrell, M. C.: The carbon dioxide (CO_2) system on the Mississippi River–dominated continental shelf in the northern Gulf of Mexico – I: Distribution and air–sea CO_2 flux, J. Geophy. Res., 120, 1429–1445, 2015.

Hunt, C. W., Salisbury, J. E., and Vandemark, D.: CO_2 Input Dynamics and Air–Sea Exchange in a Large New England Estuary, Estuar. Coast., 37, 1078–1091, 2014.

Jähne, B., Munnich, K. O., Bosinger, R., Dutzi, A., Huber, W., and Libner, P.: On parameters influencing air-water exchange, J. Geophys. Res., 92, 1937–1949, 1987.

Jiang, L. Q., Cai, W. J., and Wang, Y. C.: A comparative study of carbon dioxide degassing in river- and marinedominated estuaries, Limnol. Oceanogr., 53, 2603–2615, 2008.

Kalas, F. A., Carreira, R. S., Macko, S. A., and Wagener, A. L. R.: Molecular and isotopic characterization of the particulate organic matter from an eutrophic coastal bay in SE Brazil, Cont. Shelf Res., 29, 2293–2302, 2009.

Kirk, J. T. O.: Light and Photosynthesis in Aquatic Ecosystems, 3rd edition, Cambridge University Press, New York, 2011.

Kjerfve, B., Ribeiro, C. A., Dias, G. T. M., Filippo, A., and Quaresma, V. S.: Oceanographic characteristics of an impacted coastal bay: Baia de Guanabara, Rio de Janeiro, Brazil, Cont. Shelf Res., 17, 1609–1643, 1997.

Knoppers, B.: Aquatic primary production in coastal lagoons, in: Coastal lagoon processes, edited by: Kjerfve, B., Elsevier Science Publishers, Amsterdam, 243–286, 1994.

Knoppers, B. A., Carmouze, J. P., and Moreira-Turcqo, P. F.: Nutrient dynamics, metabolism and eutrophication of lagoons along the east Fluminense coast, state of Rio de Janeiro, Brazil, in: Environmental geochemistry of coastal lagoon systems of Rio de Janeiro, Brazil, editd by: Knoppers, B. A., Bidone, E. D., and Abrão, J. J., FINEP, Rio de Janeiro, 123–154, 1999a.

Knoppers, B., Ekau, W., and Figueiredo, A. G.: The coast and shelf of east and northeast Brazil and material transport, Geo-Mar. Lett., 19, 171–178, 1999b.

Koné, Y. J. M., Abril, G., Kouadio, K. N., Delille, B., and Borges, A. V.: Seasonal variability of carbon dioxide in the rivers and lagoons of Ivory Coast (West Africa), Estuar. Coast., 32, 246–260, 2009.

Körtzinger, A.: A significant CO_2 sink in the tropical Atlantic Ocean associated with the Amazon River plume, Geophys. Res. Lett., 30, 2287, doi:10.1029/2003GL018841, 2003.

Lee, K., Kim, T.W., Byrne, R. H., Millero, F. J., Feely, R. A., and Liu, Y.M.: The universal ratio of boron to chlorinity for the North Pacific and North Atlantic oceans, Geochim. Cosmochim. Ac., 74, 1801–1811, 2010.

Maher, D. T. and Eyre, B. D.: Carbon budgets for three autotrophic Australian estuaries: Implications for global estimates of the coastal air-water CO_2 flux, Global Biogeochem. Cy., 26, GB1032, doi:10.1029/2011GB004075, 2012.

Maher, D. T., Cowley, K., Santos, I., Macklin, P., and Eyre, B.: Methane and carbon dioxide dynamics in a subtropical estuary over a diel cycle: Insights from automated in situ radioactive and stable isotope measurements, Mar. Chem., 168, 69–79, 2015.

Matthews, H. D., Gillett, N. P., Stott, P. A., and, Zickfeld, K.: The proportionality of global warming to cumulative carbon emissions, Nature, 459, 829–832, 2009.

Mehrbach, C., Cuberson, C. H., Hawley, J. E., and Pytkowicz, R. M.: Measurements of the apparent dissociation constants of carbonic acid in seawater at atmospheric pressure. Limnol. Oceanog., 18, 897–907, 1973.

Monteiro, F., Cordeiro, R. C., Santelli, R. E., Machado, W., Evangelista, H., Villar, L. S., Viana, L. C. A., and Bidone, E. D.: Sedimentary geochemical record of historical anthropogenic activities affecting Guanabara Bay (Brazil) environmental quality, Environ. Earth Sci., 65, 1661–1669, doi:10.1007/s12665-011-1143-4, 2011.

Monteith, J. L.: Climate and the efficiency of crop production in Britain, Philos. Trans. R. Soc. Lond. Ser. B, 281, 277–294, 1977.

Nixon, S. W.: Coastal marine eutrophication: a definition, social causes, and future concerns, Ophelia, 41, 199–219, 1995.

Noriega, C. and Araujo, M.: Carbon dioxide emissions from estuaries of northern and northeastern Brazil, Scientific Reports, 4, 6164, doi:10.1038/srep06164, 2014.

Noriega, C., Araujo, M., Lefèvre, N., Montes, M. F., Gaspar, F., and Veleda, D.: Spatial and temporal variability of CO_2 fluxes in tropical estuarine systems near areas of high population density in Brazil, Reg. Environ. Chang., 15, 619–630, doi:10.1007/s10113-014-0671-3, 2014.

Orr, J. C., Fabry, V. J., Aumont, O., Bopp, L., Doney, S. C., Feely, R. a, Gnanadesikan, A., Gruber, N., Ishida, A., Joos, F., Key, R. M., Lindsay, K., Maier-Reimer, E., Matear, R., Monfray, P., Mouchet, A., Najjar, R. G., Plattner, G.-K., Rodgers, K. B., Sabine, C. L., Sarmiento, J. L., Schlitzer, R., Slater, R. D., Totterdell, I. J., Weirig, M.-F., Yamanaka, Y. and Yool, A.: Anthropogenic ocean acidification over the twenty-first century and its impact on calcifying organisms., Nature, 437, 681–6, 2005.

Paranhos, R., Pereira, A. P., and Mayr, L. M.: Diel variability of water quality in a tropical polluted bay, Environ. Monit. Assess., 50, 131–141, 1998.

Pritchard, D. W.: Estuarine Hydrography, Adv. Geophys., 1, 243–280, 1952.

Rabalais, N. N., Turner, R. E., Dıaz, R. J., and Justic, D.: Global change and eutrophication of coastal waters, ICES J. Mar. Sci., 66, 1528–1537, 2009.

Raymond, P. A. and Cole, J. J.: Gas exchange in rivers and estuaries: choosing a gas transfer velocity, Estuaries, 24, 312–317, 2001.

Rebello, A. L., Ponciano, C. R., and Melges, L. H.: Avaliacao da produtividade primaria e da disponibilidade de nutrientes na Baia de Guanabara, An. Acad. Bras. Cienc., 60, 419–430, 1988.

Reyes, E. and Merino, M.: Diel dissolved oxygen dynamics and eutrophication in a shallow well-mixed tropical lagoon (Cancun, Mexico), Estuaries, 14, 372–381, 1991.

Ribeiro, C. H. A. and Kjerfve, B.: Anthropogenic influence on the water quality in Guanabara Bay, Rio de Janeiro, Brazil, Reg. Env. Chan., 3, 13–19, 2001.

Robbins, L. L., Hansen, M. E., Kleypas, J. A., and Meylan. S. C.: CO_2 Calc: a user-friendly seawater carbon calculator for Windows, Max OS X, and iOS (iPhone), U.S. Geological Survey Open-File Report, 2010–1280, 1–17, available at: http://pubs.usgs.gov/of/2010/1280/ (last access: 6 January 2013), 2010.

Ruiz-Halpern, S., Sejr, M. K., Duarte, C. M., Krause-Jensen, D., Dalsgaard, T., Dachs, J., and Rysgaard, S.: Air-water exchange and vertical profiles of organic carbon in a subarctic fjord, Limnol. Oceanogr., 55, 1733–1740, 2010.

Rysgaard, S., Mortensen, J., Juul-Pedersen, T., Sorensen, L. L., Lennert, K., Sogaard, D. H., Arendt, K. E., Blicher, M. E., Sejr, M. K., and Bendtsen, J.: High air-sea CO_2 uptake rates in nearshore and shelf areas of Southern Greenland: Temporal and spatial variability, Mar. Chem., 128, 26–33, 2012.

Sabine, C. L., Feely, R. a, Gruber, N., Key, R. M., Lee, K., Bullister, J. L., Wanninkhof, R., Wong, C. S., Wallace, D. W. R., Tilbrook, B., Millero, F. J., Peng, T.-H., Kozyr, A., Ono, T., and Rios, A. F.: The oceanic sink for anthropogenic CO_2, Science, 305, 367–71, 2004.

Santos, V. S., Villac, M. C., Tenenbaum, D. R., and Paranhos, R.: Auto-and heterotrophic nanoplankton and filamentous bactéria of Guanabara Bay (RJ, Brazil): estimates of cell/ filament numbers versus carbon content, Braz. J. Oceanogr., 55, 133–143, 2007.

Sarma, V., Viswanadham, R., Rao, G. D., Prasad, V. R., Kumar, B. S. K., Naidu, S. A., Kumar, N. A., Rao, D. B., Sridevi, T., Krishna, M. S., Reddy, N. P. C., Sadhuram, Y., and Murty, T. V. R.: Carbon dioxide emissions from Indian monsoonal estuaries, Geophys. Res. Lett., 39, L03602, doi:10.1029/2011gl050709, 2012.

Smith, S. V., Swaney, D. P., and Talaue-McManus, L.: Carbon–Nitrogen–Phosphorus fluxes in the coastal zone: The LOICZ approach to global assessment, in: Carbon and nutrient fluxes in continental margins, edited by: Liu, K., Atkinson, L., Quiñones, R., Talaue-McManus, L., Springer-Verlag Berlin Heidelberg, Berlin, 575–586, 2010.

Souza, M., Gomes, V., Freitas, S., Andrade, R., and Knoppers, B.: Net ecosystem metabolism and nonconservative fluxes of organic matter in a tropical mangrove estuary, Piauí River (NE of Brazil), Estuar. Coast., 32, 111–122, 2009.

Stocker, T. F., Qin, D., Plattner, G. K., Tignor, M., Allen, S. K., Boschung, J., Nauels, A., Xia, Y., Bex, V., and Midgley, P. M.: Climate Change 2013: The Physical Science Basis. Contribution of Working Group I to the Fifth Assessment Report of the Intergovernmental Panel on Climate Change, Cambridge University Press, United Kingdom, 2013.

Strickland J. D. H. and Parsons T. R.: A practical handbook of seawater analysis, second ed., Fisheries Research Board of Canada Bulletin, Ottawa, Canada, 1972.

Sunda, W. G. and Cai, W. J.: Eutrophication Induced CO_2-Acidification of Subsurface Coastal Waters: Interactive Effects of Temperature, Salinity, and Atmospheric pCO_2. Environ. Sci. Technol., 46, 10651–10659, 2012.

Takahashi, T., Sutherland, S. C., Sweeney, C., Poisson, A., Metzl, N., Tilbrook, B., Bates, N., Wanninkhof, R., Feely, R.A., Sabine, C., Olafsson, J. and Nojiri, Y.: Global sea–air CO_2 flux based on climatological surface ocean pCO_2, and seasonal biological and temperature effects, Deep-Sea Res. Part II, 49, 1601–1622, 2002.

Valentin, J. L., Tenenbaum, D. R., Bonecker , A. C. T., Bonecker, S. L. C., Nogueira, C. R., and Villac, M. C.: O sistema planctônico da Baía de Gaunabara: Síntese do conheciemnto, in: Silva, S. H. G. and Lavrado, H. P., Ecologia dos Ambientes Costeiros do estado do Rio de Janeiro, Oecolog. Brasiliensis, 7, 35–59, 1999.

Villac, M. C. and Tenenbaum, D. R.: The phytoplankton of Guanabara Bay, Brazil, I. Historical account of its biodiversity, Biota Neotropic, 10, 271–293, 2010.

Wallace, R. B., Baumann, H., Grear, J. S., Aller, R. C., and Gobler, C. J.: Coastal ocean acidification: The other eutrophication problem, Estuar. Coast Shelf S., 148, 1–13, 2014.

Wanninkhof, R.: Relationship between gas exchange and wind speed over the ocean, J. Geophys. Res., 97, 7373–7382, 1992.

Weiss, R. F.: Carbon dioxide in water and seawater: the solubility of a non-ideal gas, Mar. Chem., 2, 203–215, 1974.

Wollast, R.: Evaluation and comparison of the global carbon cycle in the coastal zone and in the open ocean, in: The Sea, Vol. 10, edited by: Brink, K. H. and Robinson, A. R., John Wiley & Sons, New York, 213–252, 1998.

Yates, K. K., Dufore, C., Smiley, N., Jackson, C., and Halley, R. B.: Diurnal variation of oxygen and carbonate system parameters in Tampa Bay and Florida Bay, Mar. Chem., 104, 110–124, 2007.

Yuan, X.-C., Yin, K., Cai, W.-J., Ho, A.Y., Xu, J., and Harrison, P. J.: Influence of seasonal monsoons on net community production and CO_2 in subtropical Hong Kong coastal waters, Biogeosciences, 8, 289–300, doi:10.5194/bg-8-289-2011, 2011.

Zhai, W. D. and Dai, M. H.: On the seasonal variation of air-sea CO_2 fluxes in the outer Changjiang (Yangtze River) Estuary, East China Sea, Mar. Chem., 117, 2–10, 2009.

Zhai, W. D., Dai, M., and Guo, X.: Carbonate system and CO_2 degassing fluxes in the inner estuary of Changjiang (Yangtze) River, China, Mar. Chem., 107, 342–356, 2007.

Zhang, C., Huang, H., Ye, C., Huang, L., Li, X., Lian, J. and Liu, S.: Diurnal and seasonal variations of carbonate system parameters on Luhuitou fringing reef, Sanya Bay, Hainan Island, South China Sea, Deep-Sea Res. Pt. II, 96, 65–74, 2013.

Zhang, L., Xue, M. and Liu, Q.: Distribution and seasonal variation in the partial pressure of CO_2 during autumn and winter in Jiaozhou Bay, a region of high urbanization., Mar. Pollut. Bull., 64, 56–65, 2012.